A Numerical Investigation of E-scooter Riders' Injury Crash Mechanisms Using Finite Element Analysis

Rafael C. Chontos

Thesis submitted to the faculty of the Virginia Polytechnic Institute and State University in partial fulfillment of the requirements for the degree of

Masters of Science
In
Engineering Mechanics

Costin D. Untaroiu, Chair
Warren N. Hardy
Zachary Doerzaph

9 May 2023
Blacksburg, Virginia

Keywords: Injury biomechanics, finite element model, Electric scooter collisions, impact biomechanics,

A Numerical Investigation of E-scooter Riders' Injury Crash Mechanisms Using Finite Element Analysis

Rafael Chontos

ABSTRACT

The recent emergence of electric scooter (e-scooter) ride share companies has greatly increased the use of e-scooters in cities around the world. In this thesis, firstly, e-scooter injuries reported in the current literature as well as an overview of current e-scooter company policies, state laws, and local laws are reviewed. The most injured regions of the body were the head and extremities. These injuries are generally minor to moderate in severity and commonly include fractures and lacerations.

A primary cause of e-scooter accidents is front wheel collisions with a vertical surface such as a curb or object, generically referred to as a "stopper." Therefore, various e-scooter-stopper crashes were simulated numerically across different impact speeds, approach angles, and stopper heights to characterize their influence on rider injury risk during falls. A finite element (FE) model of a standing Hybrid III anthropomorphic test device was used as the rider model after being calibrated against certification test data. The angle of approach was found to have the greatest effect on injury risk to the rider, and it was shown to be positively correlated with injury risk. Smaller approach angles were shown to cause the rider to land on their side, while larger approach angles caused the rider to land on their head and chest. Additionally, arm bracing was shown to reduce the risk of serious injury in two thirds of the impact scenarios.

The majority of e-scooter rider fatalities (about 80%) are recorded in collisions between a car and an e-scooter. Therefore, crashes between an e-scooter and a sedan (FCR) and a sports utility vehicle (SUV) were simulated using finite element models. The vehicles impacted the e-scooter at a speed of 30 km/hr in a perpendicular collision and at 15 degrees towards the vehicle, to simulate a rider being struck by a turning vehicle. The risks of serious injury to the rider were low for the head, brain, and neck, but femur/tibia fractures were observed in all simulations. The primary cause of head and brain injuries was found to be the head-ground impact if such an impact occurred.

A Numerical Investigation of E-scooter Riders' Injury Crash Mechanisms Using Finite Element Analysis

Rafael Chontos

GENERAL AUDIENCE ABSTRACT

The recent emergence of electric scooter (e-scooter) ride share companies has greatly increased the use of e-scooters in cities around the world. In this thesis, firstly, e-scooter injuries reported in the current literature as well as an overview of current e-scooter company policies, state laws, and local laws are reviewed. The most injured regions of the body were the head and extremities. These injuries are generally minor to moderate in severity and commonly include fractures and lacerations.

A primary cause of e-scooter accidents is a scooterist hitting a small obstacle or curb. Therefore, various e-scooter crashes with an obstacle, modelled by a "stopper", were simulated using different combinations of impact speeds, approach angles, and stopper heights to understand their influence on risk of injury to the rider. The angle of approach was found to have the greatest effect on injury risk to the rider with larger angles of approach resulting in greater risks of injury to the rider. Smaller approach angles were shown to cause the rider to land on their side, while larger approach angles caused the rider to land on their head and chest. Additionally, arm bracing was shown to reduce the risk of serious injury in two thirds of the impact scenarios.

Crashes between cars and e-scooters are the cause of 80% of e-scooter rider fatalities. Therefore, crashes between an e-scooter and a sedan and a SUV were simulated to better understand the risk of injury to the rider. The vehicles impacted the e-scooter at a speed of 30 km/hr in a perpendicular collision and at 15 degrees towards the vehicle, to simulate a rider being struck by a turning vehicle. The risks of serious injury to the rider were low for the head, brain, and neck, but femur/tibia fractures were observed in all simulations. The primary cause of head and brain injuries was found to be the head-ground impact if such an impact occurred.

Acknowledgments

I would like to thank my advisor, Dr. Costin Untaroiu, for all his help and encouragement while I worked through graduate school. I would also like to thank my previous advisor, Dr. Warren Hardy, for giving a good foundation in impact biomechanics and helping find research after COVID-19 closed down a lot of opportunities. I would also like to thank Dr. Zachary Doerzaph for providing help with refining my papers to get then ready to be published. I would also like to thank Raffaella De Vita for encouraging me to apply for the GEM fellowship which helped fund my graduate career. I would like to thank Daniel Grindle for helping a great deal with debugging simulations and teaching me a lot about FE modeling.

I would like to thank my family and loved ones for encouraging me and always being supportive and interested in my research. Thank you to all my friends and lab mates for helping along the way and giving me a sense of community. Finally, I'd like to give a shout out to the MMA club at Virginia Tech and the VT Taekwondo club for being my primary stress relievers in school.

Contents

1. INTRODUCTION AND BACKGROUND

Authors: Rafael Chontos, Adam Novotny, Alexandrina Untaroiu, Zachary Doerzaph, Costin Untaroiu

Subsections 1.1 through 1.7 of this chapter were submitted as a literature review to the Journal and Transportation Engineering

1.1 ABSTRACT

The recent emergence of electric scooter (e-scooter) ride share companies has greatly increased the use of e-scooters in cities around the world. A consequence of the increase usage of e-scooters is that hospitals are reporting a significant rise in the number of injuries related to e-scooter use. This manuscript contains a review of e-scooter injuries reported in the current literature as well as an overview of current e-scooter company policies, state laws, and local laws. The most injured regions of the body were the head and extremities. These injuries are generally minor to moderate in severity and commonly include fractures and lacerations. Interestingly, although the head is one of the most commonly injured regions, helmets are not required by many states, cities, or companies when using e-scooters. Furthermore, helmet use is extremely low, even in areas that do require helmets for e-scooter operation, suggesting that stricter enforcement of e-scooter regulations may be required in the future.

1.2 INTRODUCTION

Ride share companies utilizing standing electric scooters (e-scooters) are a recent development in the United States. These companies provide two-wheeled scooters powered by electric motors that riders can rent for short term use. The rider stands on the deck of the e-scooter and engages the motor to ride around a town or city. The first e-scooter company, Scoot Networks, started in

2012. They were followed in 2017 by Lime and Bird, which are the two largest e-scooter rental companies today [14]. Despite being a relatively new form of ride share transportation, e-scooters are quickly becoming more popular and widely available [14-16]. As of 2019, over 80 cities across 26 states had standing e-scooters available [16]. As e-scooters have become more widespread and frequently used, injuries related to their use have increased [12, 14, 16]. One study found that two emergency departments in Salt Lake City saw a 625% increase in e-scooter-related injuries in the year after the launch of a ride share company when compared to the year preceding the launch [17]. Similarly, a study located in Tel-Aviv, Israel, reported a six fold increase in e-scooter-related injuries after e-scooter ride share companies were introduced [18]. Being a relatively new ride share option, e-scooter policies are still being developed [19]. At the moment, e-scooter policies vary between localities and states [11]. Also, in North America, there have been few studies related to the safety and injury mechanisms related to e-scooters, making it difficult to create evidence-based regulations to help ensure the safety of the operator [16]. This paper provides an overview of studies that have investigated standing e-scooter-related injuries and some of the regulations that e-scooter operators are supposed to abide by across the United States.

1.3 METHODOLGY

Most of the studies found in the literature about e-scooter injuries used data from 2017 to 2020. This matches with the time that popular e-scooter ride share companies were founded and e-scooters began increasing in popularity. Most papers used data from local emergency departments and had similar limitations. Company policies were gathered from Lime, Bird, Spin, Lyft, and Skip to see how they enforced safety on their e-scooters. E-scooter operating regulations from Blacksburg, VA; Austin, TX; Santa Monica, CA; and Charlotte, NC were gathered. Operating

regulations for e-scooter use in the State of California were taken from the California Vehicle Code.

1.4 ELECTRIC SCOOTER RELATED INJURIES

An overview of the injuries related to e-scooter accidents that were commonly seen in emergency departments is provided in this section. It should be noted that variations in terms of how body regions were injured and how injury types are categorized were observed in the literature. A common limitation between the studies was missing injuries that were treated outside of the emergency department [2, 11, 12, 14, 16, 20]. By only looking at trauma presented in the emergency department, there is a chance that these studies underestimated the number of e-scooter-related injuries and that the data gathered was biased towards patients with higher severity injuries [2]. Some studies may have missed patients when searching through keywords because not all hospitals had a code for e-scooter-related injuries [2, 11, 21]. In October 2020, new ICD-10-CM (International Classification of Diseases, 10th Revision, Clinical Modification) external causes codes began to be used, which should help hospitals separate injuries by the personal transportation device being operated and the cause of the injury [19]. The goal of these codes is to make it easier for researchers and traffic safety professionals to compare crash trends across all personal transportation modes [19].

1.4.1. Population Description

A large amount of literature related to e-scooter injuries provide some basic information about the sample population used, including the time-period and the number of patients with e-scooter-related injuries (Table 1). Two studies used the United States Consumer Product Safety Commission's National Electronic Injury Surveillance System to gather patient data from a sample of hospitals across the United States [12, 14]. The time periods investigated were longer for these

two studies than for other studies. Interestingly, in one study [12], the age group reported as most frequently injured was children 6 to 12 years old, while for other studies, the most frequently injured age groups were much higher (Table 1). This is most likely because the range for which data was collected ended in 2017, before e-scooter ride share companies became popular. Most ride share companies impose age restrictions on who can legally operate their scooters. In addition, nearly all e-scooter companies and localities prohibit the use of substances while operating an e-scooter. However, anywhere from 5% to 33% of patients were either confirmed or suspected of being under the influence of alcohol when injured. Although most injuries in the data sets were experienced by e-scooter riders, non-riders represented 8.4% of the injured patients observed in Trivedi, Liu et al [11]. These non-riders were injured either by tripping over a parked e-scooter or by being hit by a person riding an e-scooter [22].

Table 1: Overview of sample populations from each study.

Author(s) or Paper Title	Time Range of Interest	Sample Size	Age Data (years old)	Helmet Use	Substance Abuse
"Dockless Electric Scooter-Related Injuries Study"[2]	Sep 5, 2018–Nov. 30, 2018	190	Median: 29 Range: 9–79	< 1%	29% admitted to drinking alcohol within 12 hours of injury
Trivedi et al., 2019	Sep. 1, 2017–Aug. 31, 2018	249	Mean:33.7 Range: 8–89 10.8% under 18	4.4%	4.8% intoxicated
Puzio, Murphy et al., 2020	Sep. 4, 2018–Nov. 4, 2018	92	Mean: 30	0%	33% reported alcohol use
Aizpuru et al., 2019	2013–2017	820	Most common age range: 6–12 (34.6%)	N/A	N/A
Badeau, Carman et al., 2019	Jun. 15, 2017–Nov. 15, 2017, Jun. 15, 2018–Nov. 15, 2018	2017: 8 2018: 50	Mean: 34 Range: 18–72	0%	16% intoxicated
Farley, Aizpuru et al., 2020	2014–2019	1823	Mean: 31.3	Rare	~ 9% reported substance abuse
English, Allen et al., 2020	Sep. 5, 2018–Nov. 30, 2018	124	Median: 30	1.6%	14.5% self-reported as being intoxicated
Bloom, Noorzad et al., 2020	Feb. 1, 2018–Dec. 1, 2018	248	Mean: 35.6 Range: 9–92	3%	9% intoxicated

1.4.2. Anatomical Regions Injured

The way the body was split into different regions varied between studies (Table 2). One study used four regions: the head, the upper limbs, the lower limbs, and the chest/abdomen [2]. Another study split the leg region between the thigh and lower leg, and the arm region between the upper arm and forearm regions [14]. The head was one of the most commonly injured body regions [2, 11, 12, 14, 16, 20, 23]. The percentage of patients with head injuries varied from 17.4% [16] up to

61% [23]. Having injuries to multiple regions of the body was also common, with 48% of patients in one study having injuries to at least two different regions of the body [20].

As previously mentioned, how the extremity regions were defined and/or split varied between studies. In an Austin Public Health (APH) study, the upper limbs included the hands, wrists, arms, and shoulder [2]. In the same study, lower limbs included the legs, knees, ankles, and feet. In that study, 70% of the patients experienced upper limb injuries and 55% experienced lower limb injuries. The APH study also showed that 43% of patients experienced injuries specifically to the arms [2]. Bloom, Noorzad et al. [23] had a similar way of defining the limb regions, with one difference being that the hips were included under lower extremity injuries. Of the patients observed by these authors., 73% experienced upper extremity injuries and 62% experienced lower extremity injuries. The three most commonly injured regions observed by Aizpuru, Farley et al. [14] were the head (27.6%), the lower leg (27.3%), and the upper arm (17.7%). Injuries to the chest/abdomen were not as common [2]. The presence of alcohol caused the head and face to be more frequently injured during a crash; one study reported that sober riders fell or impacted their face/head in 54% of crashes while drunk riders impacted their head and face in 84% of crashes [24].

Table 2: Percent of patients with injuries in each body region for five studies.

Reference	Body Region			
	Head	**Upper Extremity**	**Lower Extremity**	**Multiple Regions Injured**
"Dockless Electric Scooter-Related Injuries Study" [2]	48%	70%	55%	NR
Puzio, Murphy et al., 2020	17.4%	31.8%	15.9%	12%
Aizpuru et al., 2019	27.6%	25.9%	35.1%	NR
English, Allen et al., 2020	45.5%	56.1%	34.2%	48%
Bloom, Noorzad et al., 2020	61%	73%	62%	NR

Note : NR- Not Reported

1.4.3. Types of Injuries

Some of the most common types of injuries experienced by patients were fractures/dislocations, contusions, and lacerations [11, 14, 17, 20]. Aizpuru, Farley et al. [14] found that 25.9% of patients experienced a fracture or dislocation, 25.8% experienced a contusion, and 15.2% experienced lacerations. Similarly, Trivedi, Liu et al. [11] found that 31.7% of patients experienced fractures and 27.7% experienced contusions, sprains, and lacerations. The most common location of bone fractures observed across all studies was the lower arm and wrist [11, 14, 23]. In one study, 35.4% of all fractures and dislocations were observed in the wrist and lower arm [14]. The aforementioned APH study found that nearly half of all injured riders had an injury classified as a "severe injury" [2]. Of the severe injuries, defined using The National Transportation Safety Board's definition of severe injury, 84% of those observed were bone fractures and 45% were nerve, tendon or ligament injuries [2]. As previously mentioned, head injuries are a common occurrence in e-scooter-related trauma patients. Three studies found that 13.6%–15% of all patients had evidence of, or were diagnosed with a Traumatic Brain Injury [2, 12, 16]. Trivedi, Liu et al. [11] found that 38.2% of patients experienced a minor head injury,

which was defined as a “head injury without intracranial hemorrhage or skull fracture.” The same study found that 5% of patients experienced an intracranial hemorrhage [11]. Another study found that 10.5% of patients experienced loss of consciousness at the scene [20]. Badeau, Carman et al. found that 28% of patients experienced multiple injury types, indicating that it is not uncommon for multiple types of injuries to occur as a result of an e-scooter-related incident. Finally, one study reported facial lacerations as being the single most frequent injury observed [16]. However, whereas other studies grouped all injuries of the same type together, these authors split injuries between the specific body locations and parts affected.

1.4.4. Injury Mechanisms

Several studies collected information on the mechanism of injury. A study based in Los Angeles, CA found that 80.2% of injuries were caused by falls, 11% were caused by collisions with objects, and 8.8% were caused by being hit by a moving vehicle or another moving object [11]. A study in Germany also reported that 82% of scooter crashes were caused by falls [24]. Similarly, an Austin, TX based study found that 84.7% of injuries were caused by falls, 15.3% were caused by collisions with objects, and 9.7% were caused by being hit by a moving vehicle [20]. The same study found that 4% of injuries were caused by striking a parked vehicle and 1.6% were pedestrians being hit by e-scooters [20]. English, Allen et al. [20] also determined that 15.3% of injuries involved multiple mechanisms. Another Los Angeles, CA based study found that the top three crash mechanisms were loss of balance (49%), collision between an e-scooter and automobile (14%), and uneven pavement (10%) [23]. The same study reported the speed of the e-scooter during the crash for 14% of the crashes observed in the study. In 8% of the crashes, the e-scooter was moving at a speed between 11–15 mph, in 3% of crashes, the e-scooter was moving at a speed between 6–10 mph, and in 3% of crashes, the e-scooter was moving at a speed between

0–5 mph [23]. The previously cited APH study was able to conduct interviews with many of the patients observed in that study. Through the interviews, they found that 33% of the injured patients were first time riders [2]. The interviews also revealed that 37% of the injured riders believed that excess speed may have contributed to their injury, 19% believed the injury was caused by an e-scooter malfunction, and 50% believed surface conditions were a contributing factor to their injury [2].

1.4.5. Locations of Injury Occurrence

None of the studies were able to get data on the location of the e-scooter crashes for all patients they observed. English, Allen et al. [20] reported that 70.8% of crashes occurred on the street and 3.3% occurred on the sidewalk. Similarly, the aforementioned Los Angeles, CA based study found that 36% of crashes occurred on the street, 17% occurred on the sidewalk, and for 46% of the crashes, the location was unknown [23]. Interestingly, during the time of the Los Angeles, CA study, it was illegal to operate an e-scooter on sidewalks [23]. The APH study also found that more than 55% of crashes occurred on the streets and that 33% occurred on sidewalks [2]. The same study was also able to determine that 65% of crashes occurred on a level surface and 24% occurred while traveling downhill [2]. The most common location for a collision between an e-scooter and an automobile was an intersection [25]. The two most common scooter-automobile crashes at an intersection were a car driving straight and impacting the side of an e-scooter coming from the right and a car turning right at an intersection and impacting an e-scooter coming from the car's right [25].

1.4.6. Injury Severity

The severity of the injuries experienced can be evaluated by using a recognized scoring system or looking at patient outcomes. Overall, most patients appeared to have minor to moderate injuries

and there were no fatalities [11, 14, 16, 20, 23]. One study recorded data on the Injury Severity Score (ISS) for each patient and found that the median ISS was 1, which is a low score, indicating only one body region experienced a minor injury [16]. Another study was only able to record the ISS of 24 patients and found that the median ISS was 5, indicating moderate injuries [20].

Other studies provided information on where patients went after being seen in the emergency department and what percentage had trauma activations. Table 3 shows the outcomes of the patients in three studies; in all three studies, over 90% of patients were discharged home from the emergency department after treatment [11, 14, 16]. This is what would be expected if most patients experienced mild to moderate injuries. In the three studies presented, less than 10% of patients in each study were admitted to the hospital for observation or in-patient care [11, 14, 16]. In contrast, Badeau, Carman et al. [17] found that 16% of e-scooter injury patients had to be admitted to the hospital. Similarly, Bloom, Noorzad et al. [23] found that 15% of patients had to be admitted to the hospital. Admission to the intensive care unit never exceeded 2% in any study [11, 16, 23]. Two studies found that 6% of patients were designated as trauma activations [17, 23]. Trivedi, Liu et al. [11] reported that 8.4% of the patients observed needed to have a trauma-protocol computed tomography scan. A trauma-protocol computed tomography scan is usually done when there is a high concern that a serious injury is present [11]. The same authors also reported that 70.3% of the patients observed were discharged from the emergency department within 4 hours. Lastly, these authors recorded data on Triage Acuity scores. The scores range from 1, most concerning, to 5, least concerning. A total of 61.4% of patients had a score of 4 and 23.7% had a score of 3 [11]. Additionally, drunk e-scooter riders experienced more severe injuries than sober e-scooter riders [24].

Table 3: Patient outcomes.

Reference	Outcomes (%)				
	Sent Home	**In-Patient Care**	**ICU**	**Transferred**	**Left Without Being Seen**
Trivedi et al., 2019	94%	5.2%	0.8%	N/A	N/A
Puzio. Murphy et al., 2020	91%	8%	1%	N/A	N/A
Aizpuru, Farley et al., 2019	90.8%	5.6%	N/A	1.5%	1.3%

1.5 COMPANY POLICIES

Many of the current e-scooter ride share companies have similar company policies pertaining to safety (Table 4). None of the five companies listed permits the use of electronic devices on their e-scooters or allows their e-scooters to be used under the influence of drugs/alcohol. Electronic devices are banned in order to prevent riders from operating the e-scooters while distracted [6]. All companies also limit the operation of the e-scooters to one person. Only two of the five companies evaluated require riders to wear a helmet. Bird currently only recommends that riders wear a helmet; however, they have started a program to encourage Bird scooter riders to use helmets [3]. In exchange for demonstrating helmet use while riding Bird scooters (riders upload a picture of themselves on the scooter while wearing a helmet), Bird gives out ride credits which can be used to obtain free rides later [26]. Bird also prohibits the use of Bird scooters on sidewalks unless superseded by local laws [3]. Some e-scooter companies, such as Spin and Skip, prohibit the use of their e-scooters for actions such as racing and performing stunts [6, 13]. Spin, Skip, and Lyft all forbid holding or placing any object on an e-scooter that could alter the balance of the e-scooter and thereby increase the likelihood of a crash [6, 8, 13]. Additionally, Spin and Skip both prohibit the use of their e-scooters during inclement weather or when other potential hazardous environmental conditions are present [6, 13]. Lastly, a rule that appeared to be unique to Spin was

that closed toed shoes or sneakers are required to be worn while operating the e-scooter [6]. Some companies also set service hours when their scooter can be operated. Lime has service hours between 7 a.m. and 8 p.m. [27]. Similarly, Lyft has service hours set to 2 hours before sunrise until 2 hours after sunset [27].

Table 4: Company safety policies.

Company	Helmet Use	Minimum Age (years)	Driver's License or ID	Electronic Device use	Substance Use	Number of Riders Allowed
Lime [1]	R	18, 16 with supervision	R	B	B	1
Bird [3]	E	18	R	B	B	1
Spin [6]	R	18	R	B	B	1
Lyft [8]	Re	18	R	B	B	1
Skip [13]	Re	18	NM	B	B	1

Note R – Required, Re – Recommended, E – Encouraged, B – Banned, NM – Not mentioned.

1.6 GOVERNMENT REGULATIONS

With the rapid proliferation of e-scooters, may regions have crated specific regulations governing their use. This section describes the laws and regulations at local and state levels. No federal regulations specific to e-scooters were identified.

1.6.1. City Laws

The laws between different cities regarding e-scooter use vary. Table 5 shows a small portion of common laws on e-scooter operation found in four cities or towns. As seen in the table, all cities require e-scooter operators to be sober, obey traffic laws, and be the only individual on the scooter [4, 5, 7, 9, 10]. However, the regulations on helmet use, where an e-scooter can be used, and the maximum speeds at which they can be operated vary.

In Blacksburg, VA, helmets are recommended but not required, even on the university campus at Virginia Tech [4, 28]. If an e-scooter is being operated on a street, it is subject to motor vehicle speed laws [5]. On off-street bike trails, e-scooters may go faster than 15 mph [5]. E-scooters are prohibited from being used on the streets or sidewalks of Downtown Blacksburg [4]. On Virginia Tech's Blacksburg campus, e-scooters are allowed on sidewalks if the riders are careful and give pedestrians the right of way [28]. Texting or having earphones in both ears is prohibited [4, 28].

In Santa Monica, CA, all e-scooter riders must wear a helmet [7]. E-scooters are only permitted to be used in the bike lanes of streets and cannot be used on sidewalks [7]. This law is in contrast with the other cities reviewed, which allow e-scooters to be operated on sidewalks. E-scooters have a maximum speed limit of 15 mph [7]. Although no law explicitly sets a minimum age for operating an e-scooter, operators are required to have a driver's license or permit, effectively making the minimum age of operation 15.5 years [7].

In Austin, TX, only riders under 18 years old are required to wear a helmet, although helmet use is still recommended for older riders [9]. The City of Austin allows e-scooters to be operated on streets and sidewalks provided operators ride safely on sidewalks [9]. There is not a speed limit set by the City of Austin on e-scooter operation [9]. E-scooter riders are required by the City of Austin to go with the flow of traffic [9].

In Charlotte, NC, e-scooter riders 16 years and younger are required to wear a helmet, while riders older than 16 years are only encouraged to wear a helmet [10]. As is the case in Santa Monica, CA, the City of Charlotte has a maximum speed limit of 15 mph for e-scooters [10]. E-scooters can be operated on the streets and on sidewalks except those where e-scooters are prohibited [10].

Table 5: Local laws on e-scooter operation.

City/Town	Helmet Use	Locations of Use	Obey Traffic Laws	Maximum Speed (mph)	Substance Use	Number of Riders Allowed
Blacksburg, VA [4, 5]	Re	NA (Downtown)	Yes	15 on off-street bike paths	B	1
Santa Monica, CA [7]	R	Only in bike lanes	Yes	15	B	1
Austin, TX [9]	R (under 18 years old)	Sidewalks if done safely	Yes	NM	B	1
Charlotte, NC [10-12]	R (under 16 years old)	NA (on certain sidewalks)	Yes	15	B	1

Note: R – Required, Re – Recommended, B – Banned, NM – Not mentioned

1.6.2. California Laws

The laws e-scooter riders must follow in the state of California were reviewed because California was one of the earliest states to adopt e-scooter ride share systems [11]. California sets the maximum speed for e-scooters at 15 mph [29]. E-scooters can be used on roads with speed limits of 25 mph or less except in places where local authorities have chosen to allow e-scooters on roads with speed limits up to 35 mph [29]. Currently, riders under the age of 18 years must wear a helmet [29]. Before January 1, 2019, helmets were required for all e-scooter riders; however, California passed legislation that removed the restriction for those 18 years and older [23]. Similar to the cities outside of California discussed in the previous section, e-scooters can only be ridden by one person and operators must have a valid driver's license [29]. E-scooters cannot be used on sidewalks and the operator cannot carry any object that prevents them from holding the handle bars [29]. A unique California rule is that a person riding an e-scooter cannot

position the handle bars in a way that would require them to raise their hands above their shoulders [29].

1.7 DISCUSSION

As e-scooter ride share companies are becoming more popular, the number of patients with e-scooter related injures is increasing [12]. This can be seen via studies comparing the number of patients with e-scooter related trauma from before and after the introduction of ride share companies. One study observing patients visiting an emergency department in Indianapolis, IN from September 4, 2018, to November 4, 2018, found 92 patients had e-scooter related injuries [16]. When observing the same period for 2017, before e-scooters were available in Indianapolis, there were zero patients with e-scooter related injuries. A similar study based in Salt Lake City, UT, found that there was a 625% increase in patients with e-scooter related injuries [17]. Farley, Aizpuru et al. found that the estimated emergency department visits related to e-scooters increased from 4,881 in 2014 to 29,268 in 2019. More specifically, the estimated e-scooter related emergency department visits increased from 8,269 in 2017 to 15,522 in 2018 just one year after the Bird and Lime companies started [12].

E-scooter injury patients' ages are also interesting, as many of the e-scooter companies set the minimum age for e-scooter use at 18 years, yet several studies had patients under 18. In one case, 10.8% of the patients observed were under the age of 18 [11]. Another study based in Los Angeles, CA, reported that 6% of patients were under the state mandated legal operating age of 16, and 9% were under the companies' mandated minimum age of 18 [23].

During the study's time frame, California had a law mandating helmet use on e-scooters but only 3% of patients wore helmets [23]. A Santa Monica, CA based study observed people operating scooters and found that 94% of riders did not use a helmet and 26% of riders used e-

scooters on sidewalks where they were banned [11]. Tandem riding was observed in 7.8% of riders and 9.3% of riders did not comply with traffic laws [11]. An Austin, TX based study found that the median weight of patients injured while operating an e-scooter was 82 kg with 22.6% of the patients weighing more than 100 kg, the maximum recommended weight of most ride share e-scooters [20]. These studies indicate that improvements in enforcing both company policies and government laws are needed.

To encourage safe riding practices, Bird has started a "helmet selfie" program to encourage helmet use, but there has not been a study on how effective this program has been on increasing helmet use [26]. One study found that the mean speed of e-scooters used was 5.46 mph, with a minimum speed of 1 mph and a maximum speed of 24.96 mph [15]. The same study found that 60% of the trips lasted less than 10 minutes and 65% of the trips spanned less than 1 mile [15]. The length and duration of a typical trip match what would be expected of a mode of transportation being used for "last mile" transportation.

As indicated in previous sections, the most common cause of e-scooter injuries was falling off the e-scooter. Some of the common injuries experienced by riders were fractures/dislocations and contusions. The head, upper limbs, and lower limbs were the most common places for injuries to occur. Despite this, and against the recommendation and regulations of local governments and companies, riders rarely chose to wear helmets. A recent study has shown that bicycle helmets were effective in reducing most head injury metrics except head angular acceleration [30]. Unfortunately, even with the reduced injury metrics, the authors calculated a high risk of severe head injuries for e-scooter riders [30]. This suggests that future studies should research how to improve the current design of bicycle helmets with e-scooter crashes in mind.

1.8 OBJECTIVES AND CHAPTER SUMMARY

The purpose of this thesis was to explore the link between crash mechanism and injury outcomes for various different e-scooter crash scenarios. The impact simulations created also tested how different pre-impact variables effected the injury outcomes. This work provided useful insights in the link between crash mechanism and injury outcome and can be used as a reference from which computational methods for studying injury outcomes may be further developed. Chapters 2 and 1, excluding section 1.8, have been submitted for publication at the time of this writing. Similarly, chapter 3 is expected to be submitted for published within a week of this writing. The chapter titles and summaries are:

Chapter 2. A Numerical Investigation of Rider Injury Risks During Falls Caused by E-scooter-Stopper Impacts:

This chapter focused on the development of a FE model of an e-scooter and used a FE model of a standing Hybrid III dummy to model the rider. The Hybrid III model was calibrated as part of this study and used to explore the effect of approach angle, stopper height, and impact speed on injury outcome. This work has been submitted for publication in the Journal of Biomechanical Engineering and is under review.

Chapter 3. A Numerical Investigation of E-scooter-to-Vehicle Traffic Accidents:

This chapter discussed using a Global Human Body Models Consortium simplified male 50^{th} percentile finite element model to explore the injury risks associated with intersection impacts between a car and an e-scooter rider.

Chapter 4. Conclusion:

This chapter discussed the limitations and main conclusions of this thesis.

2. A NUMERICAL INVESTIGATION OF RIDER INJURY RISKS DURING FALLS CAUSED BY E-SCOOTER STOPPER IMPACTS

Authors: Rafael Chontos, Daniel Grindle, Alexandrina Untaroiu, Zachary Doerzaph, Costin Untaroiu

This chapter was submitted as a research paper to the Journal of Biomechanical Engineering in November 2022

2.1 ABSTRACT

Within the past decade, injuries caused by electric scooter (e-scooter) crashes have significantly increased. A primary cause involves front wheel collisions with a vertical surface such as a curb or object, generically referred to herein as a stopper. In this study, various e-scooter-stopper crashes were numerically simulated across different impact speeds, approach angles, and stopper heights to characterize their influence on rider injury risk during falls. A finite element (FE) model of a standing Hybrid III dummy was used as the rider model, after being calibrated against certification test data. Additionally, an FE model of an e-scooter was developed based on reconstructed scooter geometry. Forty-five FE simulations were run to investigate various e-scooter crash scenarios. Test parameters included impact speed (3.2 m/s up to 11.16 m/s), approach angle (30° up to 90°), and stopper height (52 mm, 101 mm, and 152 mm). Additionally, the perpendicular (90°) impact scenarios were run a second time with arm activation added into to the model to mimic the rider attempting to catch themselves. Overall, the risks of serious injury to the rider varied greatly; however, roughly half of the impact scenarios indicated serious risk to the rider. This was expected, as the speeds tested were in the upper 25th percentile of reported scooter speeds. The angle of approach was found to have the greatest effect on injury risk to the rider and

it was shown to be positively correlated with injury risk. Smaller approach angles were shown to cause the rider to land on their side while larger approach angles caused the rider to land on their head and chest. Additionally, arm bracing was shown to reduce the risk of serious injury in two-thirds of the impact scenarios.

2.2 INTRODUCTION

Since 2012, ride share companies in the United States have offered standing two-wheel electric scooters (e-scooters) for public short-term rental [14]. Various companies allow people to rent out e-scooters for commuting or recreation, thereby eliminating the need for the population to purchase, store, and maintain a scooter themselves. Despite being relatively new, these ride-share companies have quickly increased the popularity, use, and availability of e-scooters [11, 14, 16].

The increase in e-scooter use has also led to an increase in e-scooter traffic injuries [16]. The injuries observed were generally mild to moderate in severity and occurred most frequently to the head and limbs [11, 14, 16, 31]. The most common types of injuries to the body were fractures, dislocations, and contusions [11, 14, 17, 20]. From the available literature, the most common mode of crash appeared to be falls and were single vehicle crashes involving only the rider of the e-scooter [11, 20, 32, 33]. A Los Angeles, CA based study found that 80.2% of injuries were caused by falls [11]. The same study also found that collision with an object caused 11% of crashes and collision with a vehicle or other moving object caused 8.8% of crashes [11]. Similarly, a Swedish study found that 83% of scooter crashes involved only the scooter rider and 12% involved other road users, such as cars or other scooter riders [33].

The field of e-scooter injury research is relatively new and limited, especially regarding computational crash recreation. Much of the current literature focuses on observing injury trends reported by emergency rooms, but not the biomechanical causes of these injuries. Experimental

and modeling-based research on the topic is sparse and has only examined either pothole-based falls [34] or rigid body impacts where the scooter-rider drove into a stationary vehicle [35]. While these studies are insightful, they used rigid-body rider models and were limited in their selection of pre-impact variables. Specifically, the researchers in the pothole impact study recommend varying the angle of approach because the study only used head-on collision scenarios [34]. Notably, neither study investigated how an attempt by the rider to catch themselves might change the injury risks [34, 35].

The objective of this study was to investigate the biomechanical causes of trauma associated with e-scooter crashes resulting in fall events across a range of pre-impact conditions. These falls were created by numerically simulating a rider falling off an e-scooter after impacting a vertical transition referred to as a "stopper" (i.e., curb or another rigid object). To investigate this event, a finite element (FE) model of an e-scooter was developed and the Hybrid III Dummy model (HIII), an anthropometric test device (ATD) currently used in automotive impact regulations, acted as an e-scooter rider to simulate falls. This study will be among the first to use a deformable rider model to explore the effect of various e-scooter pre-impact conditions and their effect on rider safety and will lay the foundation for further e-scooter fall research.

2.3 METHOD

To investigate e-scooter crashes, models of an e-scooter, a road, and a stopper were created. The three pre-impact variables examined in this study were impact speed, stopper height, and approach angle. Additionally, the simulations that modeled a head on collision (90° approach angle) were run a second time with arm muscle activation to simulate a rider attempting to catch themselves.

2.3.1 Development of an E-scooter FE Model

The scooter geometry was created by scanning a Spin (SPIN, San Francisco, CA) Ninebot KickScooter MAX electric scooter using a FARO laser scanner system [6]. The initial geometry was smoothed and transformed into a Non-uniform rational B-spine (NURBS) surface in Rhino 3D (Robert McNeel & Associates, Seattle, WA) and then imported to be meshed in Hypermesh (Altair, Troy, MI, USA). Finally, the scooter mesh was imported into LS-PrePost (LSTC/Ansys, Cannonsburg, PA, USA) where the scooter parts were defined, and their material properties assigned based on literature data (Figure 1). In this model, all parts of the scooter were rigid except for the tires.

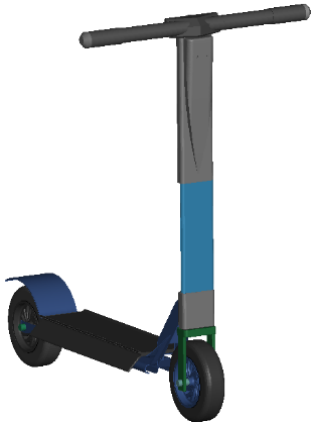

Figure 1. Spin electric scooter FE rendering.

The e-scooter tire shells were modelled using a piecewise linear plasticity material and inflated like an airbag [36]. The scooter was connected with 13 rigid body constraints and two joint revolute constraints. The two joint revolute constraints were used on the rods that connect the font tire to the front arm and the rear tire to the deck to allow the rods to spin with the tires. The wheel supports were in between the tire shell and the rims. The electric scooter was 1,110 mm tall and 1,008 mm in length. The deck of the scooter was 536 mm by 205 mm and the handlebars had a 680 mm span. The wheels had an inner radius of 69 mm, an outer radius of 111 mm, and a thickness of 60 mm.

2.3.2 Calibration of a Hybrid III FE Model

Currently, there are several detailed FE human body available (e.g., THUMS, GHBMC, etc.) used in automotive safety, but due to their high computational cost they are used mostly for simulations of the collision phase, when the human model interacts with the vehicle parts (around 150-200 ms). In comparison, a multibody dynamics (MBD) human model approximates roughly a certain human geometry (using ellipsoids) and is used mostly to predict the human kinematics during the impact due to its possible inaccuracies in modeling the contact. For example, for the impacts which required large computational time (e.g. a collision with the pre-crash phase), the pre-impact phase is simulated with rigid body models whose kinematics is transferred before impact to the detailed human FE model [37]. Due to time consuming and complexity of the e-scooter–bumper simulations, where the impact with the ground could occur at different time depending on the initial pre-impact configuration, it was decided to model the scooter rider on the whole simulation (around 0.8 -1 s) using a computational efficient FE model of a standing Hybrid III dummy (Ansys/LSTC) in LS-Dyna [38]. This dummy FE model represents a 50th percentile male (78.1 kg, 1700 mm height), and its mesh is relatively coarse containing 4,301 elements and 7,355 nodes.

While no validation data of this dummy model was available, various body parts of a Hybrid III model were verified against certification test data [39]. If the certification results were not in the corresponding test corridors, the dummy parts were calibrated by changing the original parameters of their material models. Four certification tests were used in this study: the head drop test, the neck extension and flexion test, the knee impact test, and the thorax impact test [38-40]. The contact between impactors and dummy segments was modeled using an automatic surface to

surface contact with soft constraint formulation to take into account the differences in mesh size and stiffness between dummy and impactor parts in contact [41].

The certification test of the head was a drop test of the Hybrid III head dummy [39]. To simulate this test, the head portion of the dummy model was isolated and placed directly over a meshed ground (Figure 2a). The head was then given an initial velocity of -2.716 m/s in the vertical direction to simulate the head being dropped from a height of 376 mm. The specifications required that peak resultant acceleration of the center of the gravity of the head, filtered using SAE filter class 1000, to be in a range between 225 G and 275 G [39]. The resultant acceleration curve was also required to be unimodal [39]. The final specification that the head needed to match was that the peak lateral acceleration be between -15 G and 15 G [39]. The calibration process was performed using a design of experiments (DOE) optimization approach in LS-Opt (Ansys/LSTC). The elastic bulk modulus, the short-time shear modulus and the long-time shear modulus of the head skin material model were defined as design variables and were defined with ranges which included the original values of the current head skin material model (*MAT_VISCOELASTIC, Material type 6). The difference between the peak head acceleration and 250 G (the middle of the corridor) were minimized, while a constraint between -15 G and 15 G was added for the peak lateral acceleration. A sequential adaptive modelling optimization with domain reduction was used to calibrate the head FE model with respect to design variables in four iterations. In this approach, the possible designs to be simulated were chosen using a space filling DOE scheme in LS-Opt. After each iteration, a radial basis function metamodel was developed. Based on the metamodel, the optimum design after each iteration and new points to be simulated were derived using the metamodel by an adaptive simulated annealing, a global stochastic optimization algorithm that mimics the metallurgical annealing process.

In the neck certification test, the assembly of the neck and head components were attached to a rigid pendulum [42] (Figure 2b). The pendulum was released from certain heights to generate desired velocities (6.96 m/s in flexion and 6.06 m/s in extension) and impacted a deformable aluminum stopper. The y-direction moments measured at the neck joint should be in certain ranges for flexion (47-58 Nm) and extension (88-108.4 Nm) tests. The calibration simulation did not model the free fall of the pendulum, instead the corresponding pre-impact angular velocities were assigned to the rigid pendulum. Additionally, deceleration pulses were assigned to the pendulum to simulate the impact with the aluminum stopper. The parameter of stiffness curve in the neck-head joint were defined as the design variable and the extension/flexion peak moments were constrained to be in the certification ranges. The optimization process was similar to the corresponding process used in the head drop calibration.

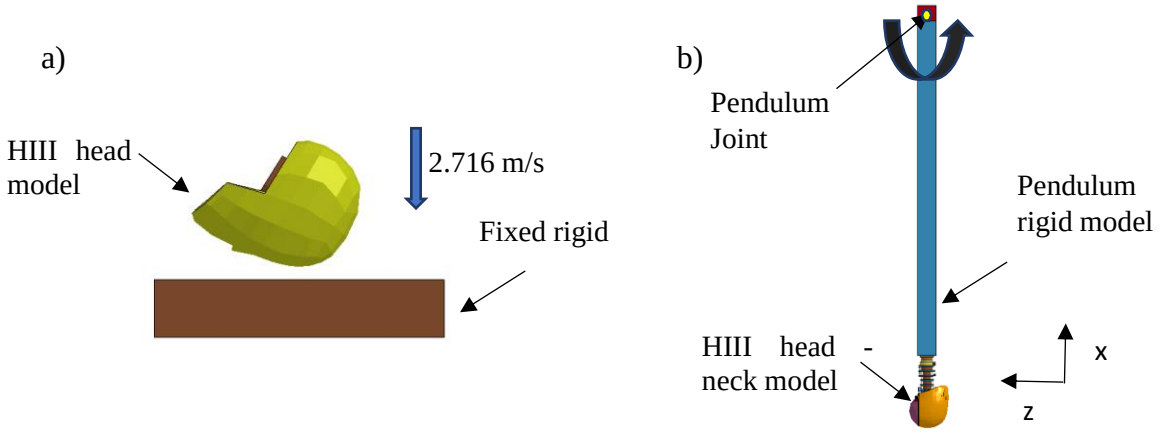

Figure 2. The calibration of HIII finite element Model: a) Head in drop impact b) Neck-Head in pendulum simulation.

In the thorax certification test (Figure 3a), the whole dummy was seated without back support on a rigid surface. A 23.38 kg cylinder with 152.32 mm diameter and 6.7 m/s initial velocity frontally impacted the dummy's chest. The two outcomes that were calibrated were chest compression and peak resistance force. The maximum chest compression needed to be between

63.5 and 72.6 mm [38]. Similarly, the peak resistance force was required to be between 5.16 and 5.894 kN [43]. LS-Opt was used to calibrate the thorax by changing the Young's modulus of the rib and bib parts of the dummy thorax.

The upper and lower legs were calibrated to a frontal knee impact test (Figure 3b). The lower leg was isolated from the dummy and positioned to match the knee impact test set up for a Hybrid-III dummy described in the Humanetics model [39]. The upper leg was fixed in space. The knee impactor had a mass of 4.998 kg and a diameter of 76.2 mm and impacted the knee with a velocity of 2.1 m/s. The maximum peak impact force had to be between 4.715 and 5.782 kN [39]. The response of original knee model was in the test corridor; therefore, no changes were made.

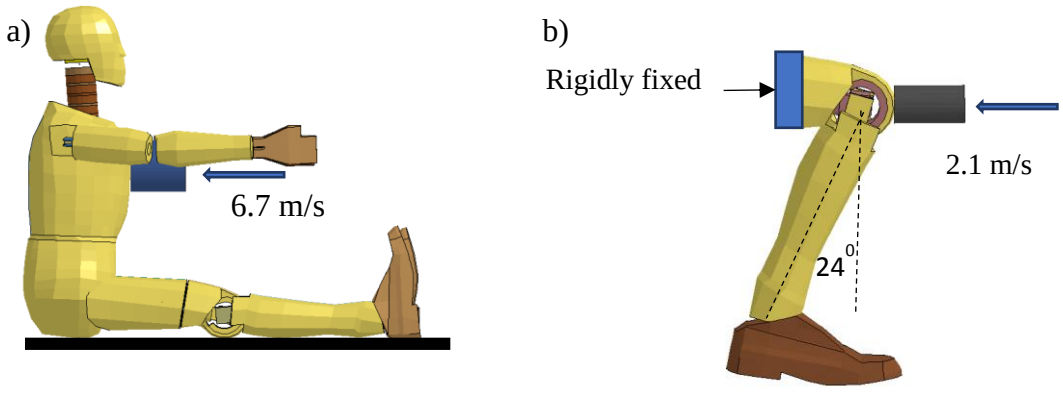

Figure 3. The calibration of HIII finite element Model: a) Thorax in pendulum impact b) Knee pendulum impact.

2.3.3 E-scooter-stopper Impact Simulations

To model an e-scooter crash, the calibrated HIII FE model was placed on the e-scooter model (Figure 4). The hands and feet were constrained to the scooter using the COONSTRAINED_ JOINT_LOCKING keyword card [41]. The release times of the feet and hands were adjusted based on the time of impact between the scooter and the stopper. The feet and hands were released slightly 6 ms after the moment of wheel-stopper impact. The ground was modeled as a deformable

asphalt structure using the LS-Dyna material card 159 MAT_CSCM_CONCRETE [44]. The contact between the dummy and ground was modeled using the automatic_surface_to_surface contact card [41]. The soft contact option was enabled and set to 1 for soft constraint formulation. Additionally, the static coefficient of friction was set as 0.85 and the dynamic coefficient was set as 0.6.

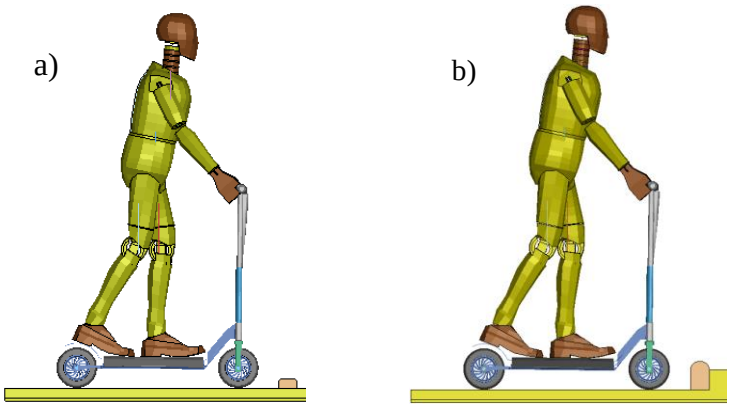

Figure 4. The scooter set up for a) stopper height of 52 mm and an approach angle of 90° and b) stopper height of 152 mm and an approach angle of 90°.

A DOE study was used to investigate the effect of impact speed, stopper height, and approach angle on rider injury risks. The impact speeds used in this study were 3.2 m/s, 4.48 m/s, and 11.16 m/s. These speeds were chosen based on reported operation speeds of e-scooters [15]. The linear velocity of the scooter and dummy was achieved using initial velocity generation and initial velocity rigid body keyword cards. Both the dummy and the scooter were given the same initial linear velocity. An angular velocity was applied to wheels of the scooter using initial velocity keyword cards. This made the wheels spin as they would on a moving scooter. The stopper heights examined were 52 mm, 101 mm, and 152 mm. The first two stopper heights were chosen to simulate the scooter impacting small obstacles or bumps (Figure 4a) that can be present on the sidewalks, bike lanes, and streets on which e-scooters are typically operated [2, 20, 23]. The last

stopper height was selected because 152 mm is the height of a typical curb [45]. The ground after the 152 mm stopper was raised to mimic how the ground after a curb is generally higher than the street (Figure 4b). Finally, the approach angles tested were 90°, 60°, 45°, and 30°. The approach angle was the angle between the line of travel of the scooter and the obstacle (Figure 5). A Latin hypercube scheme was used to generate 36 crash scenarios.

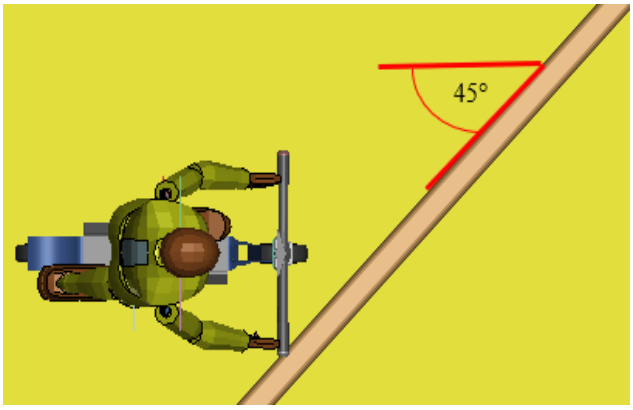

Figure 5. The initial set up for a 45° approach angle.

Nine additional simulations were run using a perpendicular initial collision configuration (90° approach angle). In these additional simulations the Hybrid III was modeled attempting to break its fall with its hands. To simulate arm activation, the dummy's shoulder and elbow joints were loaded directly after the wheel-stopper impact, which caused the arms to rotate forward simulating a rider trying to catch themselves with their hands (Figure 6). The results from the arm activation simulations were directly compared to same simulations without arm activation to observe how the arm activation affected the risk of injury.

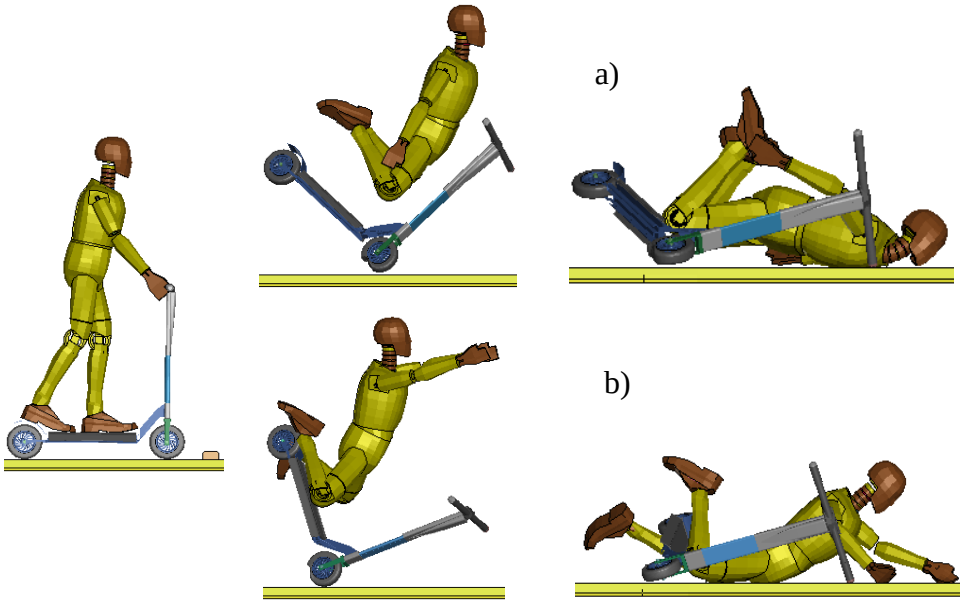

Figure 6. The dummy falling a) without arm activation and b) with arm activation.

Risk probabilities of body region AIS 3+ (serious) injuries were calculated based on head injury criteria (HIC), neck injury criteria (NIC), chest deflection, and maximum femur force [46]. These probabilities were used to calculate the rider injury measure (RIM), as an overall likelihood of serious injury to the rider (Table 6). The brain injury criteria (BrIC) was not examined in this study because the presence of evidence of traumatic brain injury in scooter crash patients was 15% or lower [2, 12, 16] and the Hybrid III dummy has not been tested for BrIC outcomes.

The Pearson product-moment correlation coefficients between DOE variables and the probability of injuries were calculated to measure the strength of the relationship between different crash pre-impact conditions and injury risks. The correlation coefficients were calculated by importing the pre-impact conditions and resulting injury risks from each simulation into LS-Opt. In addition, the global effects of each pre-impact variable on the risk of injury was examined using Sobol's global sensitivity analysis in LS-Opt [47]. When combined with the information obtained from the correlation coefficient, the sensitivities provided insight on which variables had the

largest impact on rider injury. Student t-tests were calculated to determine if arm activation caused statistically significant changes in injury outcomes. In this statistical test, called also null-hypothesis significance testing (NHST), a p-value is calculated and if $p \leq \alpha=0.05$ [48], it is typically considered to be statistically significant (the null hypothesis is rejected). However, it should be mentioned that NHST has several shortcomings [49], so NHST tests can only be considered preliminary (exploratory) heuristics [49]. The simulation set that used a head on impact with a stopper height of 52 mm and impact speed of 3.2 m/s was excluded from the t-tests because it was an outlier.

Table 6. Calculation of Injury Criterion

Injury metrics	Risk Function	Ref
HIC_{15} (AIS3+)	$P_{HIC} = \Phi\left(\frac{\ln(HIC_{15}) - 7.45231}{0.73998}\right)$	[50]
N_{ij} (AIS3+)	$P_{N_{ij}} = \frac{1}{1+e^{3.227-1.969*N_{ij}}}$	[51]
Chest Deflection (AIS3+)	$P_{chest} = \frac{1}{1+e^{10.5456-1.568*(\delta_{max})^{0.4612}}}$	[50]
Femur Compression (AIS3+)	$P_{femur} = \frac{1}{1+e^{4.9795-0.326*FemurForce}}$	[50]
RIM (AIS3+)	$1-(1-P_{HIC})*(1-P_{BrIC})*\left(1-P_{N_{ij}}\right)*(1-P_{chest})*(1-P_{femur})$	[50]

2.4 RESULTS

The final e-scooter model contained a total of 392,450 elements and 387,966 nodes. All of the scooter parts except for the tire shells were modelled using a rigid material model for steel [52].

The calibration of the HIII pedestrian dummy's body regions was successfully performed. After material property calibration, the HIII's head, neck, and torso reported test outcomes within the certification range. The original HIII's leg models were not altered because their responses were

in the knee certification range. Original and calibrated test data is presented in the appendix (Figures A1-4).

A wide range of RIM scores—ranging from 0.08–1.0 (Table B1)— were observed across the simulations. In concurrence with reported injuries, the most injured body regions were the head and neck [11, 14, 16]. Notably, in 10 of the 11 simulations that reported RIM > 0.9, HIC was the largest regional injury measure and typically by a large margin. Head injury AIS3+ risks were above 25% in 16 out of 36 simulations. Neck injury risks were above 25% in 18 out of 36 the simulations. Chest injury risks were above 25% in 2 of the 36 simulations. Femur injury risks were below 25% in all simulations.

Approach angle had the largest influence on all four injury outcomes, reporting 56–91% of sensitivities (Figure 7a). The correlation coefficients, determined using the Analysis of Variance (ANOVA), a linear sensitivity measure implemented in LS-Opt, indicated that larger approach angles were strongly correlated with larger head (0.602), neck (0.615), chest (0.648) and overall (0.627) injury risks (Figure 7b). Approach angle had a small negative association with risk of femur injury (-0.19). Four of the five lowest RIM simulations used the smaller approach angles of 30° and 45°. Furthermore, nearly all the simulations with a RIM of 1.0 used a 90° approach angle.

Impact speed had the second largest effect on injury measures, with sensitivity values between 5% and 30%. Impact speed was slightly negative correlated with RIM (-0.025) and chest injury (-0.062), but positively correlated with head (0.066), neck (0.121), and femur (0.263) injury. Speed had the largest effect on femur injury risks even though femoral injury risk never rose above 21.7%.

Stopper height had the smallest effect on injury measures, with sensitivity values between 3% and 16%. Stopper height had a moderately negative correlation with RIM (-0.307), suggesting that larger heights reported smaller RIM values (Fig. 7b). Stopper height was negatively correlated with head (-0.205) and neck (-0.073) injury risks but was positively correlated with femur (0.144) and chest (0.045) injury risks.

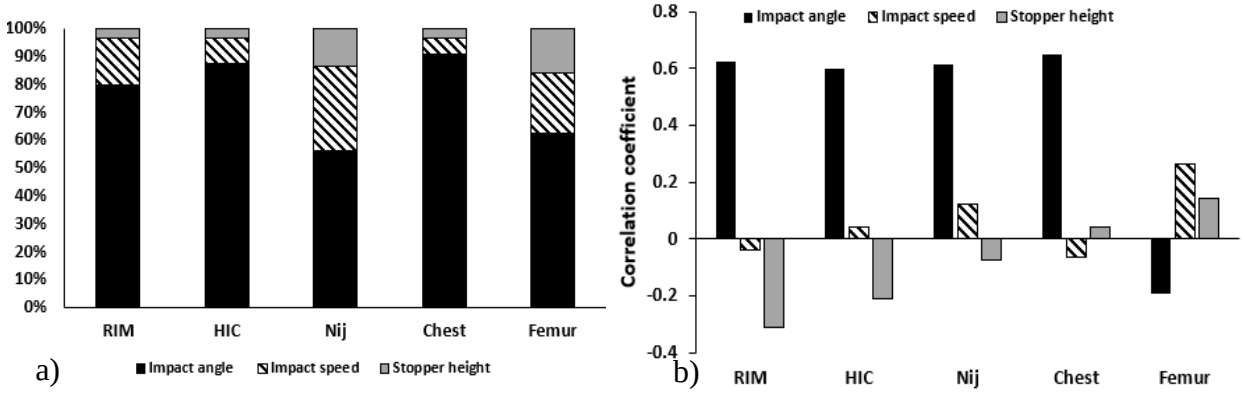

Figure 7. Sensitivity of Injury risks to pre-impact variables a) Global Sensitivity Approach/Sobol b) Linear Sensitivity Approach / ANOVA.

Dummy arm activation caused varying effects on injury risks (Table C1). Six of the nine simulations resulted in reduced RIM scores when arms were activated. RIM typically decreased because of lower head, neck, and chest injury risks. Dummy arm activation had a statistically significant effect on the neck injury risk ($p = 0.042$), a less significant effect on RIM ($p = 0.065$) and HIC ($p = 0.064$), and an insignificant effect on chest ($p = 0.119$) and femur ($p = 0.32$) injuries.

2.5 DISCUSSION

This study is amongst the first to examine e-scooter falls with a deformable rider model and a variety of pre-impact conditions. In addition to the development of an FE e-scooter, an FE model of the HIII pedestrian was calibrated. The calibrated HIII showed responses in the corridors of

certification tests, suggesting the dummy model can be used by the safety community in car-to-pedestrian simulations.

Compared to a recent study performed to investigate the falls of e-scooter riders caused by potholes [34], this study investigated a larger group of speeds, different stopper heights, and considered possible rider arm activation during the contact to the ground. Furthermore, the current study included the angle of approach as variable which had a significant effect on RIM. Finally, a finite element approach was used which has more accurate contact modeling compared to the rigid-body approach used by other groups [34]. Another recent study used various angles of approach, however that study focused mainly on the head and comparing the risk of severe head injuries for a rider wearing a helmet and a rider without a helmet [30]. In contrast, the current study observed injuries across the entire dummy and specifically looked at how changing the angle of approach and arm activation affected the fall kinematics and RIM.

The pre-impact condition with the largest impact on rider injury risk was the angle of approach. Perpendicular impacts (90°) reported substantially larger injury risks than impacts at 30–60°. Impact speed and stopper height, in the ranges investigated in this study, played small roles in injury risk outcomes. The surprisingly low correlation of the scooter speed with head/RIM injury risk may be partially explained because the injuries are caused mostly by the vertical head impact with the ground (caused by gravity), not by the horizontal velocity. Similar findings have been observed for pedestrian ground contact injuries [53]. The recorded RIM values varied between 0.08 and 1.0. About half of the RIM scores indicated a high risk of serious injury to the rider despite many reported injuries resulting from e-scooter use being mild to moderate in severity. This was not surprising as the speeds tested were in the upper 25th percentile for reported e-scooter usage speeds [15].

Approach angle may have had the largest effect on injury measures because the angle of approach largely determined how the rider fell and which parts of the body hit the ground first. In a 90° impact, the dummy fell or flew forward. For example, in the high-speed 90° impact, the flung dummy's head hit the ground first, resulting in large HIC and RIM values (Figure 8). In the lower speed 90° impacts, the knees hit the ground first and the dummy collapsed forward with the chest and head contacting the ground at high angular velocities. In contrast, an approach angle of 30° caused the rider to land on their side and shoulder first. In most cases, the head of the HIII dummy did not contact the ground at all, resulting in a lower HIC and RIM (Figure 9). RIM did not increase in these shoulder-first impacts because only anterior-posterior chest deflection was examined, and thus any risk of lateral chest deflection-based injuries was not incorporated.

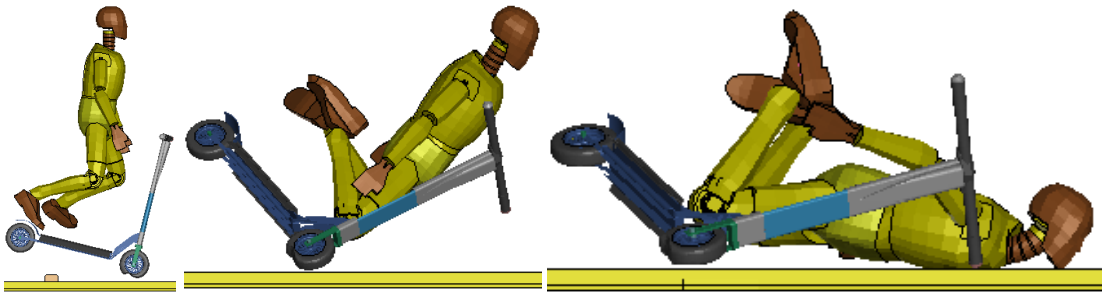

Figure 8. 90° approach angle, 52 mm stopper, 11.16 m/s impact without arm activation.

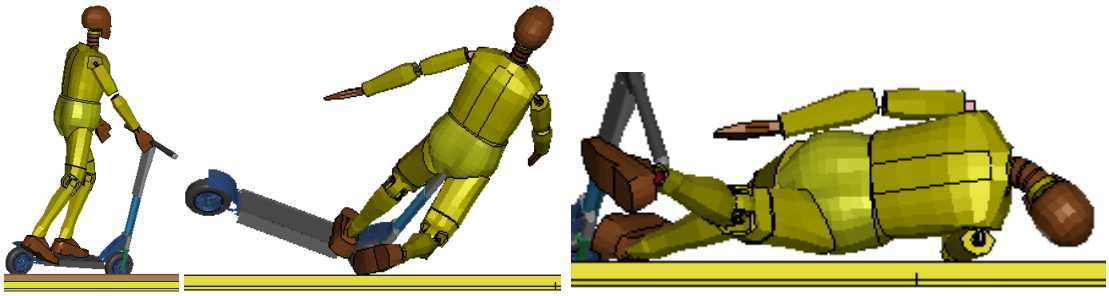

Figure 9. 30° approach angle, 52 mm stopper, 11.16 m/s impact without arm activation.

A surprising result of the study was the small and negative correlation between impact speed and RIM. However, when the simulations were grouped such that the only variable changed in

each group was speed (Table C2), a trend emerged between the sign of the correlations and the angle of approach for the group. For angles of attack of 60° and 90°, impact speed had a primarily positive correlation with injury risk. For angles of attack of 45° and 30°, impact speed had a primarily negative correlation with injury risk. This trend could be attributed to the angle of approach changing the kinematics of the fall. For collisions involving higher angles of approach, the dummy landed with its chest and head facing the ground and speed had the expected positive correlation with injury risk. However, for smaller angles of approach, the dummy landed primarily on its side where little to no injury risks were observed. Thus, the direction the dummy impacted the ground may have played a larger role on impact outcomes than did speed.

Interestingly, the dummy attempting to catch itself did not reduce the risk of serious injury as much as initially expected. This was primarily caused by the kinematics of the fall varying between each simulation and the dummy being unable to mimic exactly how a person would respond while falling. For example, in the case of a head-on collision with a 52 mm stopper at 3.2 m/s and arm activation, the dummy catches itself and then bounces before eventually having its head contact the ground, resulting in large HIC values (Figure 10). In this specific case the HIC is higher than the no arm activation case, causing the RIM to increase. However, a person may not have impacted the ground after successfully catching themselves or may have adjusted their arms to brace for the second impact. A scenario such as this might cause a greater reduction of the risk of injury to the neck and head regions, which were usually the biggest contributors to the RIM for the rider. Because of the unusually large increase in RIM, this specific simulation set was excluded from the t-test calculation.

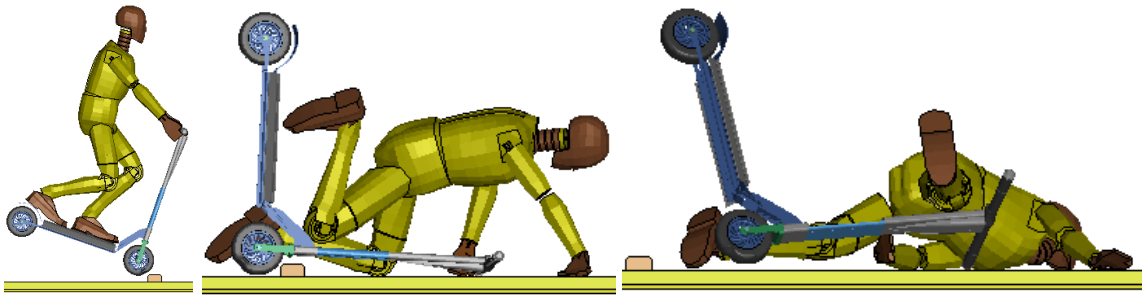

Figure 10. 90° approach angle, 52 mm stopper, 3.2 m/s impact with arm activation.

This study was limited in its selection of injury measures. The RIM equation only examined head, neck, anterior-posterior chest, and femoral injury risks. This technique excluded potential injuries caused by lateral-medial chest compression. Not including this injury measure caused the chest injury risk for simulations where the dummy landed on its side to be unrealistically small since only anterior-posterior deflection was examined (Figure 9). In addition, upper extremity injuries were not examined in this study despite being reported in e-scooter falls. These injury measures were excluded because the HIII dummy model had not been calibrated for these loading scenarios. Future work should use a rider model that can better capture more injury measures to further explore e-scooter falls. For example, replacing the coarse HII dummy FE model with a detailed or simplified human pedestrian FE model (e.g., GHBMC, THUMS) [54-56], which include more impact validations (e.g. in lateral plane), may provide more biofidelic responses and should be investigated in the future. The rider's kinematic s during the fall phase may be influenced significantly by the wheel-bumper impact and the time when the rider's hands are disconnected from the scooter handlebars. Therefore, additional validation of the rider-scooter models is recommended when physical collision data will be available.

An additional limitation to this study was its impact speed selection. This study only examined impacts with linear initial velocities, while real e-scooter riders experience crashes and falls during turning or braking events. These different initial velocity and acceleration conditions may result

in rider kinematics not seen in this study. Future work should examine the turning events and braking events prior to crashes and falls to better investigate e-scooter safety. The final limitation to this study was that a HIII dummy is used for frontal impacts and not designed for impacts to the side of the dummy. To verify the results of this study, a future study should look run the low approach angle crash scenarios with a rider model better suited for side impacts.

2.6 CONCLUSION

This study simulated 45 e-scooter crashes caused by an impact with a stopper and examined the effect of impact speed, approach angle, and stopper height on the risk of serious injury to the rider. The study found that the angle of approach was the dominant variable in determining the risk of injury to the rider. The approach angle had a positive correlation with injury risks in the head, neck, chest, and femur regions. Approach angle affected the kinematics of the dummy's fall, which caused the head to contact the ground, resulting in large head and neck injury risks. Surprisingly, impact speed had a weak but generally positive correlation with injury risk. Arm activation was added for the head-on collision simulations to mimic a person attempting to catch themselves. In two-thirds of the simulations, arm activation resulted in a slightly lower risk of regional injuries. This was likely due to the simplified arm activation model technique made to mimic a person catching themselves. Overall, this study successfully explored the effect of various pre-impact variables that may prove useful to future bio mechanists studying e-scooter safety. The work serves as a reference from which computational methods for studying injury outcomes resulting from scooter crashes may be further developed, providing a useful tool for exploring scooter designs, protective equipment, deployment strategies, and policies.

2.7 CHAPTER APPENDIX

Appendix A. HII's Responses in Certification Tests

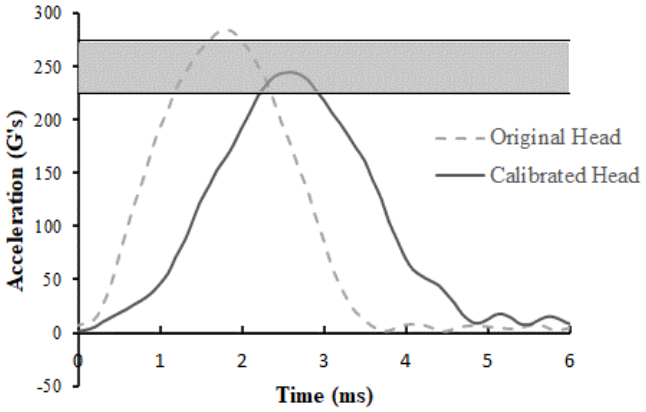

Figure A1. The calibration of HIII head in drop impact simulation.

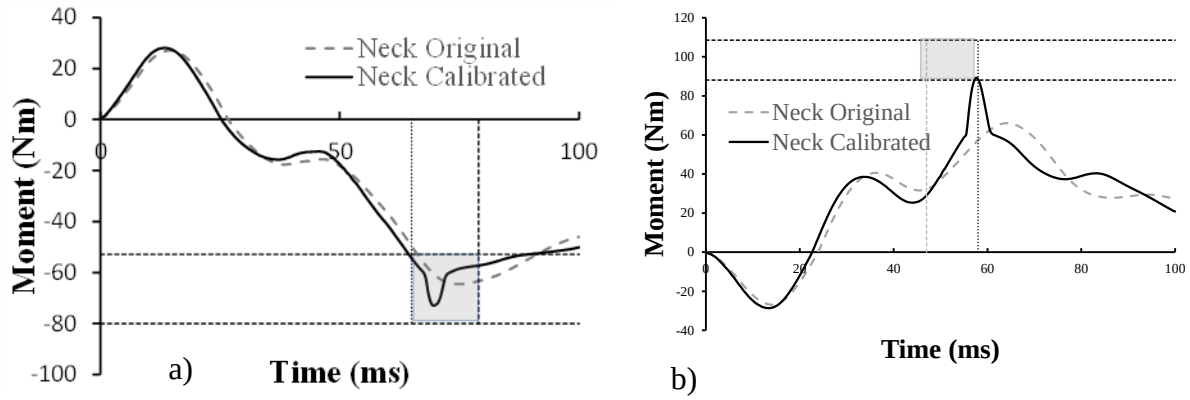

Figure A2. The calibration of HIII neck impact simulation: a) Extension, b) Flexion.

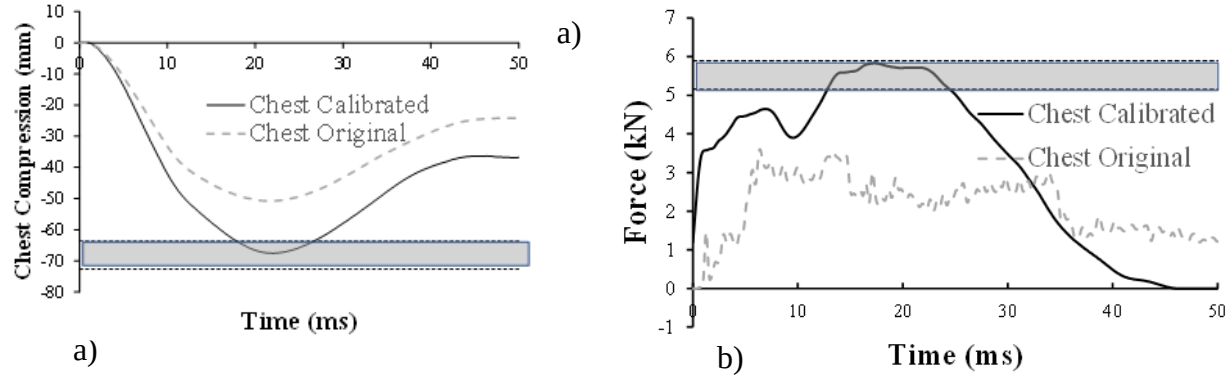

Figure A3. The calibration of HIII chest in pendulum impact simulation. a) chest compression b) chest impact force.

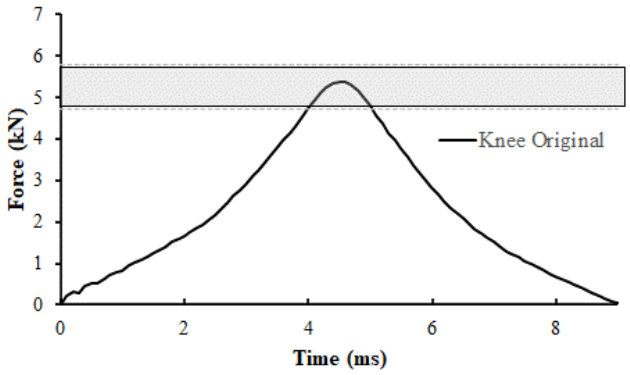

Figure A4. The verification of HIII knee in pendulum impact simulation.

Appendix B. DOE Results

Table B1. Probability of Serious Injury – Whole Body and Regional Injuries

Case	Approach angle	Stopper height (mm)	Velocity (m/s)	RIM	HIC	Nij	Chest	Femur
1	90	52	3.20	0.496	0.173	0.271	0.152	0.014
2	60	52	3.20	0.961	0.946	0.257	0.001	0.02
3	45	52	3.20	0.974	0.97	0.117	0.001	0.024
4	30	52	3.20	0.08	0	0.063	0	0.018
5	90	101	3.20	0.86	0.782	0.33	0.026	0.015
6	60	101	3.20	0.645	0.426	0.368	0.003	0.018
7	45	101	3.20	0.145	0.001	0.124	0.001	0.022
8	30	101	3.20	0.101	0	0.081	0	0.019
9	90	152	3.20	1	0.999	0.645	0.149	0.015
10	60	152	3.20	0.083	0	0.066	0	0.018
11	45	152	3.20	0.112	0	0.091	0	0.023
12	30	152	3.20	0.087	0	0.07	0	0.017
13	90	52	4.48	0.772	0.995	0.461	0.112	0.014
14	60	52	4.48	0.738	0.165	0.667	0.004	0.054
15	45	52	4.48	0.451	0.177	0.323	0.001	0.014
16	30	52	4.48	0.815	0.343	0.661	0.136	0.041
17	90	101	4.48	1	1	0.379	0.295	0.024
18	60	101	4.48	0.348	0.22	0.142	0.001	0.024
19	45	101	4.48	0.7	0.545	0.326	0.003	0.018
20	30	101	4.48	0.975	0.961	0.354	0.002	0.035
21	90	152	4.48	0.966	0.67	0.845	0.328	0.028
22	60	152	4.48	0.088	0	0.071	0	0.018
23	45	152	4.48	0.111	0	0.09	0	0.022
24	30	152	4.48	0.09	0	0.073	0	0.019
25	90	52	11.16	1	1	0.499	0.176	0.036
26	60	52	11.16	1	0.999	0.234	0.001	0.022
27	45	52	11.16	0.087	0	0.07	0	0.018
28	30	52	11.16	0.109	0	0.086	0	0.025
29	90	101	11.16	1	0.999	0.967	0.001	0.029
30	60	101	11.16	0.999	0.994	0.813	0	0.036
31	45	101	11.16	0.122	0	0.105	0	0.019
32	30	101	11.16	0.108	0	0.093	0	0.016
33	90	152	11.16	0.999	0.97	0.94	0.216	0.025
34	60	152	11.16	0.249	0.156	0.092	0	0.021
35	45	152	11.16	0.086	0	0.072	0	0.015
36	30	152	11.16	0.093	0	0.072	0.001	0.217

Appendix C. Correlation Coefficients

Table C1. Risk of Serious Injury for Head-on Impact Simulations

	Arm Activation	RIM	HIC	Nij	Chest	Femur
Case I $(90°, 52\ mm, 3.2\ m/s)$	No	0.49	0.17	0.27	0.15	0.01
	Yes	0.88	0.85	0.16	0.001	0.01
Case II $(90°, 101\ mm, 3.2\ m/s)$	No	0.86	0.78	0.33	0.03	0.01
	Yes	0.12	0	0.09	0.001	0.03
Case III $(90°, 152\ mm, 3.2\ m/s)$	No	1	0.99	0.64	0.15	0.01
	Yes	0.80	0.75	0.20	0	0.02
Case IV $(90°, 52\ mm, 4.48\ m/s)$	No	0.77	0.51	0.46	0.11	0.01
	Yes	0.91	0.84	0.28	0.24	0.03
Case V $(90°, 101\ mm, 4.48\ m/s)$	No	1	1	0.37	0.295	0.02
	Yes	0.76	0.68	0.24	0.01	0.04
Case VI $(90°, 152\ mm, 4.48\ m/s)$	No	0.96	0.67	0.84	0.33	0.03
	Yes	0.93	0.89	0.42	0.01	0.02
Case VII $(90°, 52\ mm, 11.2\ m/s)$	No	1	1	0.49	0.17	0.04
	Yes	1	1	0.48	0.26	0.03
Case VIII $(90°, 101\ mm, 11.2\ m/s)$	No	1	0.99	0.96	0.001	0.03
	Yes	0.84	0.18	0.80	0.002	0.03
Case IX $(90°, 152\ mm, 11.2\ m/s)$	No	0.99	0.97	0.94	0.22	0.03
	Yes	0.43	0.003	0.40	0.02	0.03

Table C2. Correlation Coefficients Between Impact Speed and Injury Risk (No Arm Activation Cases)

	RIM	HIC	Nij	Chest	Femur
Case A $(90°, 52\ mm)$	0.91	0.96	0.74	0.68	0.99
Case B $(60°, 52\ mm)$	0.49	0.41	-0.40	-0.50	-0.31
Case C $(45°, 52\ mm)$	-0.89	-0.75	-0.52	-0.99	-0.29
Case D $(30°, 52\ mm)$	-0.33	-0.36	-0.33	-0.36	-0.05
Case E $(90°, 101\ mm)$	0.62	0.62	0.99	-0.43	0.88
Case F $(60°, 101\ mm)$	0.81	0.92	0.88	-0.78	0.98
Case G $(45°, 101\ mm)$	-0.40	-0.36	-0.43	-0.49	-0.49
Case H $(30°, 101\ mm)$	-0.36	-0.36	-0.34	-0.29	-0.46
Case I $(90°, 152\ mm)$	0.34	0.29	0.84	0.01	0.43
Case J $(60°, 152\ mm)$	0.99	0.99	1	0.98	1
Case K $(45°, 152\ mm)$	-0.99	0.98	-0.99	0.93	-0.99
Case L $(30°, 152\ mm)$	0.88	0.98	0.31	0.99	0.99
Overall	-0.03	0.066	0.121	-0.06	0.263

3. A NUMERICAL INVESTIGATION OF E-SCOOTER-TO-VEHICLE TRAFFIC ACCIDENTS

Authors: Rafael Chontos, Daniel Grindle, Zachary Doerzaph, and Costin Untaroiu

This chapter will be submitted to the journal of Computer Methods in Biomedical Engineering in May 2023

3.1 ABSTRACT

Within the past decade, injuries caused by electric scooter (e-scooter) crashes have significantly increased. A common cause of fatalities for e-scooter riders is a collision between a car and an e-scooter. To develop a better understanding of the complex injury mechanisms in these collisions, four crashes between an e-scooter and a family car/sedan and a sports utility vehicle were simulated using finite element models. The vehicles impacted the e-scooter at a speed of 30 km/hr in a perpendicular collision, and at 15 degrees towards the vehicle, to simulate a rider being struck by a turning vehicle. The risks of serious injury to the rider were low for the head, brain, and neck, but femur/tibia fractures were observed in all simulations. The primary cause of head and brain injuries was found to be the head-ground impact in cases where such an impact occurred.

3.2 INTRODUCTION

Since 2012, ride share companies in the United States have offered standing two-wheel electric scooters (e-scooters) for public short-term rental [14]. Various companies allow people to rent e-scooters for commuting or recreation, thereby eliminating the need for users to purchase, store, and maintain a scooter themselves. Despite being relatively new, these ride-share companies have quickly increased the popularity, use, and availability of e-scooters [11, 14, 16].

The increase in e-scooter use has also led to an increase in e-scooter traffic injuries [16]. Since their inception, observed e-scooter injuries have generally been mild to moderate in severity and occurred most frequently to the head and limbs [11, 14, 16, 31]. The most common types of injuries to the body were fractures, dislocations, and contusions [11, 14, 17, 20]. While generally mild injuries, 80% instances where riders were killed were caused by vehicle collisions [57].

The field of e-scooter injury research is relatively new, especially in terms of computational crash studies. Much of the current literature has focused on observing injury trends reported by emergency rooms, but not the biomechanical causes of these injuries. Experimental and modelling-based research on the topic is sparse. Researchers from Knoxville, TN reported that 67% of collisions between an e-scooter and an automobile occurred at an intersection [25]. Despite this prevalence of impacts, only one study has investigated the biomechanics of this impact scenario. A previous computational study examined a sedan laterally impacting a stationary e-scooter rider [58]. While this novel study was insightful, it used an unvalidated vehicle model to impact the rider model, did not examine the injuries resulting from the rider-ground interaction, and the only variable altered was the posture of the rider. To better investigate and improve rider safety, additional impact simulations should be completed using validated vehicle models, consideration for ground impacts, and a wider variety of impact conditions.

The objective of this study was to investigate the biomechanical causes of rider injuries in intersection vehicle impacts across a wider range of pre-impact conditions using finite element models (FE). This study will be among the first to use a deformable rider model and validated vehicle model to investigate e-scooter rider injury risks and will expand the knowledge of vehicle-rider injury outcomes. This study is the first to examine the underlying biomechanics of e-scooter rider injuries in vehicle impacts.

3.3 Method

To investigate scooter-car crashes, a previously developed e-scooter model was acquired [59]. The scooter rider was modelled with the Global Human Body Models Consortium (GHBMC) simplified 50th percentile male pedestrian model (M50-PS) [60]. The GHBMC M50-PS was selected to increase the pedestrian model's biofedelity relative to other low-computation options such as the Hybrid-III model, developed primary to be used in frontal crashes, which the authors have used previously for investigating scooter collisions. The GHBMC was positioned on the e-scooter to mimic a typical e-scooter rider stance (Figure 11) [61].

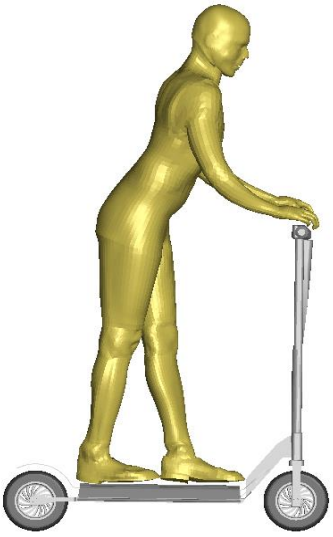

Figure 11. The GHBMC model positioned on the scooter.

Two publicly available and validated vehicle models were used to impact the rider: a family car/sedan (FCR) and a sports utility vehicle (SUV) [62]. The two different vehicle types (low profile and high profile) increased the breadth of potential rider outcomes [62]. The original windshield models were rigid, but using a rigid model would have created unrealistic rider-windshield interactions; thus, the windshield was made deformable. The deformable windshield was modelled as a dual layer windshield with the top layer modelled as glass and the bottom layer

modelled as polyvinyl butyral, or PVB [63]. The ground was modelled as deformable asphalt, as was done in a previous FE rider injury study [59]. An initial linear velocity of 3.2 m/s was applied to the scooter and rider, and the vehicle had an initial speed of 30 km/h with 1 gravity of braking acceleration. Rider position relative to the car has been examined in previous work, so only the most dangerous posture was examined in this study. The rider posture used in this study posed the GHMBC model with one foot on the front of the deck and the other foot placed behind the front foot on the back of the deck. The rider was slightly bent forward. This posture was used because it is the most common riding posture [61]. There were two primary types of intersection vehicle-rider impacts [25]. The first type was a vehicle traveling straight through the intersection and impacting a rider coming from the motorists' right side [25] (**Error! Reference source not found.**). This typology accounted for 31% of intersection collisions [25]. The second common crash type accounted for 29% of intersection collisions. This was a motorist turning right at an intersection and a scooter again coming from the right of the motorist [25].

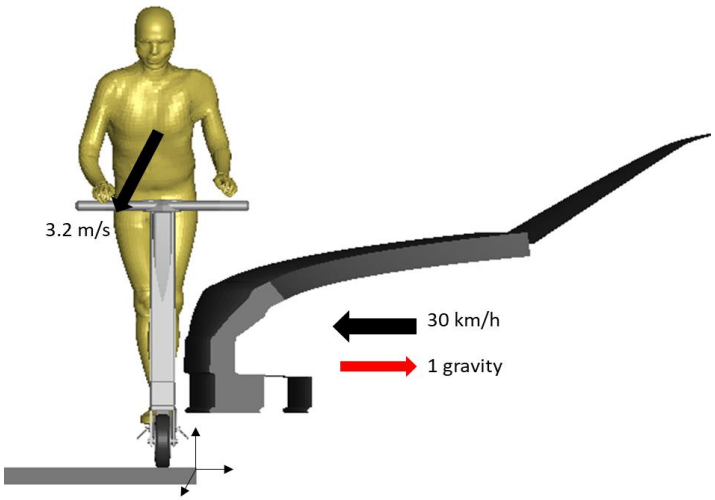

Figure 12. The setup of a model of a sedan vehicle impacting the left side of the scooter rider.

These two impact types were modelled by adjusting the angle of the scooter 15 degrees to mimic a scooter rider being impacted by a turning vehicle (Figure). Although this study focused on impacts to the left side of the car, two right side impacts were run and showed similar results to the left side scenarios.

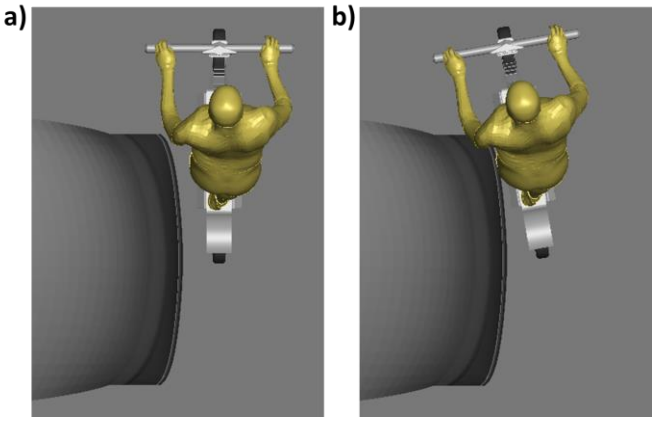

Figure 13. A head on collision a) and b) an angle impact collision**.**

The impact simulations were run on the Virginia Tech Advanced Researching Computing cluster in LS-DYNA (version 10.2). Simulations were run until the rider model hit and then rested on the ground. The probability of serious injury (Abbreviated Injury Scale [AIS] 3+) was calculated using injury outcomes from the head injury criteria (HIC), brain injury criteria (BrIC), neck injury risk (Nij), femur injury risk, and tibia fracture risk (Table 7).

Table 7. Injury risk functions

Injury metrics	Risk Function	Ref
HIC_{15} (AIS3+)	$P_{HIC} = \Phi\left(\frac{\ln(HIC_{15}) - 7.45231}{0.73998}\right)$	[46]
BriC (AIS3+)	$P_{BrIC} = 1 - e^{-\left(\frac{BrIC}{0.987}\right)^{2.84}}$	[46]
N_{ij} (AIS3+)	$P_{N_{ij}} = \frac{1}{1 + e^{3.227 - 1.969 * N_{ij}}}$	[51]
Femur Fracture Risk	$P_{Femur} = \frac{1}{1 + e^{4.9795 - 0.326 * F}}$	[46]

Tibia Fracture Risk	$P_{Tibia} = \frac{F}{F_c} + \frac{\sqrt{M_x^2 + M_y^2}}{M_c}$	[64]

Lower extremity component failure (element elimination) was permitted in these simulations. If element erosion was observed in the tibia or femur, the injury risk was recorded as 1.

3.4 RESULTS AND DISCUSSION

All four impacts reported tibia and femur fracture (Figure 14). The risk of neck injury was low across all the impacts (neck risk < 0.05). Three out of the four impacts resulted in low head and brain injury risks, but the straight SUV impact reported more substantial risks (head risk = 0.56, brain risk = 0.22).

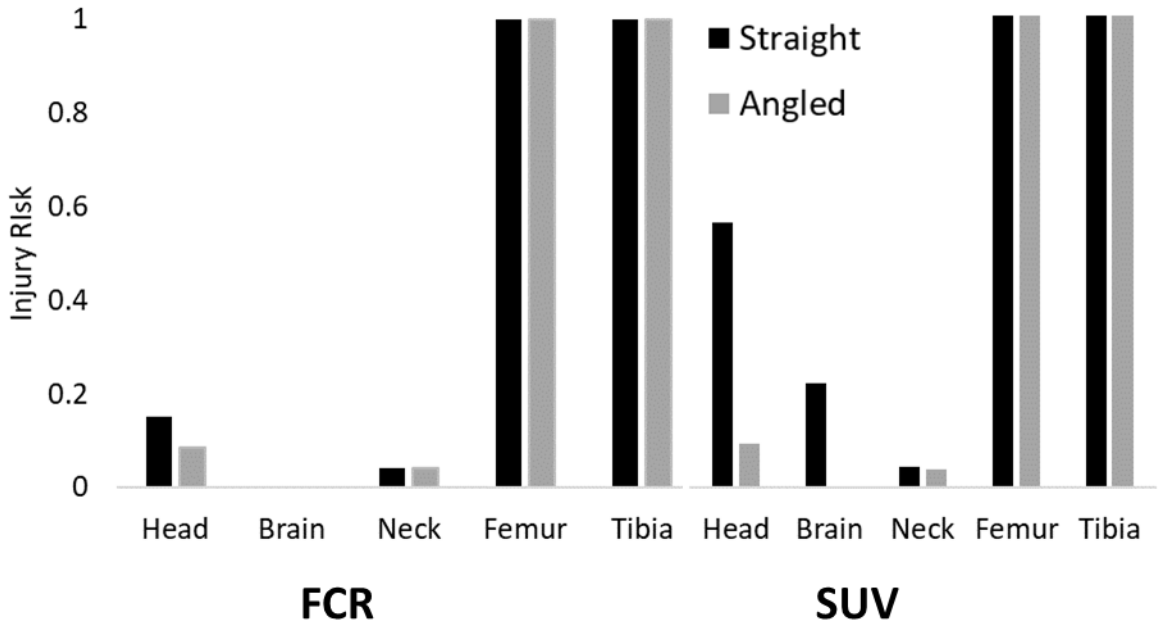

Figure 14. Injury risks to the rider based on region.

In three of the four impacts, the head, brain, and neck reported low injury risks due to a lack of head-vehicle or head-ground contact. In these impacts, the rider's head never hit the vehicle; instead, the rider rolled forward and separated from the vehicle (Figure 15). In addition, for these impacts, the rider impacted the ground first with the legs and arms, breaking the fall and reducing

the intensity of the head-ground contact. In two impacts, the head never hit the ground due to the arms breaking the fall.

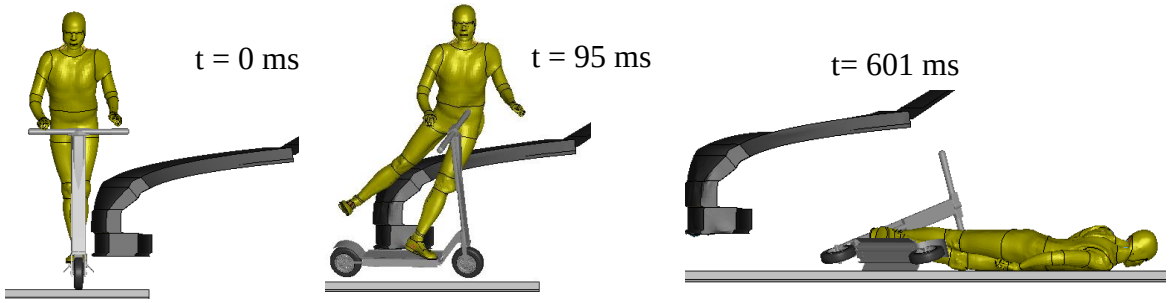

Figure 15. Rider kinematics with minimal head injury (FCR-Straight).

The SUV-Straight impact reported larger head and brain injury risks because the rider's head contacted the ground (Figure 16). In this impact, the rider flipped over the hood of the SUV and impacted the ground headfirst, resulting in large head and brain injury risks. These results suggest that to properly protect the rider, head-ground contact must be softened, as the vehicle impact was not the cause of life-threatening injury.

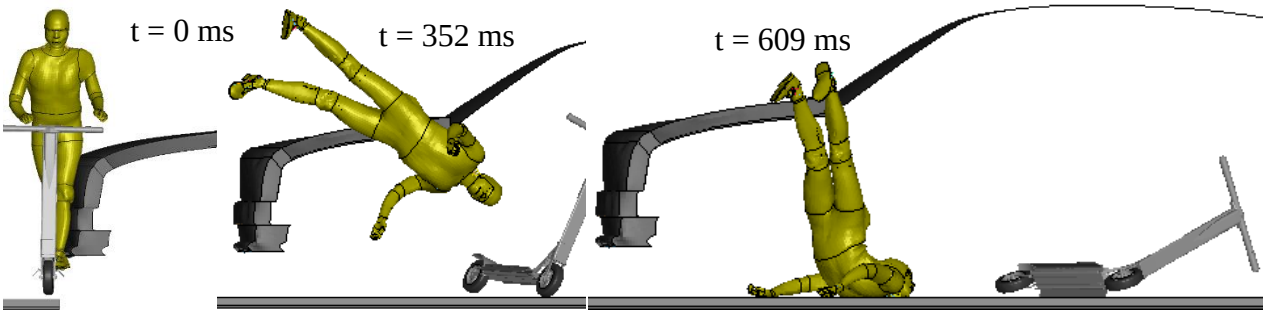

Figure 16. Rider kinematics with minimal head injury (SUV-Straight).

The head, brain, and neck injuries reported in this study matched reported rider injuries in vehicle collisions but the tibia and femur injuries were larger than as reported in injury surveys [25]. One possible reason for this leg injury discrepancy is that the vehicle impact velocity in most intersection crashes may be lower than what was modelled in this study. It is likely that smaller impact velocities would reduce the risk of serious injuries to the femur and tibia.

This study was limited by its lack of muscle activation. It is likely a rider would attempt to break their fall in an impact. This arm motion and muscle activation may alter the kinematic impact response and potentially change the injury outcomes. For example, a shielding of the head may have prevented the large head injury risk in the SUV-Straight impact (Figure 16). Future work should examine the effect of bracing and shielding on impact outcomes.

In addition to a lack of muscle activation, this study was limited in its pre-impact conditions. A single impact speed was explored. To capture a wider range of rider kinematic and injury responses, vehicle impact speed and rider initial velocities should be varied.

3.5 CONCLUSION

This study simulated four vehicle to e-scooter impacts using an FCR and SUV across two different impact angles. The tibia and femur were fractured in all four impacts, but the head, brain, and neck typically experienced minimal injuries. The primary cause of head and brain injuries came from the head-ground contact, which only occurred in one of the four impacts. This suggests that rider-ground protection should be prioritized over rider-vehicle protection, as it was reported in car-to-pedestrian impacts at low car velocities [65]. However, additional crash conditions informed by real world crash reports should be undertaken to confirm this finding.

4. CONCLUSION

4.1 LIMITATIONS AND FUTURE WORK

Finite element models of 50^{th} percentile standing male dummies were used in the thesis to exam injuries risk to a scooter rider during a variety of crash scenarios. The main limitations of this study were the human model selection, muscle passivity, and injury criterion selection.

Only a FE model of a 50th percentile male was used in this study. Although the median weight for injured riders was about 82 kg, over 20% of rider weighed over 100kg [20]. Also, 30% to 50% of injured riders were female [2, 11, 14, 16, 17, 20, 23, 66]. This shows a gap in the current research as most studies have focused on male riders. Additionally, height, weight and sex have been shown to affect injury outcomes in car-pedestrian collisions [67, 68]. Future e-scooter crash studies should use different anthropometries to observe what effect, if any, rider height, weight, and sex have on injury outcomes.

Most of the crash simulations in this study used passive models. Generally, people would react to falling or being crashed into. As shown in Chapter 2 of this thesis, the way a person reacts can affect the injuries experienced by the rider. The passive models in this study should be expanded by including muscle activation to observe how a rider reacting to the crash effects the injury outcomes. Additionally, the muscle activation used in Chapter 2 was a rudimentary attempt to model a rider attempting to catch themselves. This muscle activation is a great starting point but should be refined an improved in future studies. Lastly, the simulations in this study focused on risk of serious injury to the rider and did not look into arm injuries. As arm are one of the most commonly injured regions of the body, future studies should create simulation use rider models capable of outputting arm injure/fracture risk.

4.2 CONCLUSION

In this thesis a finite element model of a male 50th percentile standing Hybrid III dummy was calibrated and used in scooter-bump crash simulations. A way to model muscle activation was developed and applied to select simulations in the scooter-bump collisions. In addition, a simplified finite element model of a male 50th percentile GHBMC model was used to model a scooter rider in scooter-car crash scenarios. The results of the scooter-bump simulations showed

that in scenarios where the rider falls of the scooter the head is the most likely region of the body to be injured. In a scooter-bump scenario, should the rider fail to react to the fall it was discovered that they would very likely to experience serious injuries to the head and neck. The rudimentary arm activation reduced the risk of serious injury to the rider's head and neck too. Interestingly, the scooter-bump collision showed that for a fall scenario the angle of approach was the most significant factor in determining the likelihood of serious injury and the location of injury occurrence. The scooter-car impacts results in serious injuries to legs of the riders, however showed primarily low risks of serious injuries to the head and neck of the rider. The work presented in this study helped link crash mechanisms to injuries which can be expanded further in future studies.

REFERENCES

[1] Lime. "Rules & Regulations." Lime. https://help.li.me/hc/en-us/articles/360001546234-Rules-Regulations (accessed January 3, 2021).

[2] Austin Public Health, "Dockless Electric Scooter-Related Injuries Study," Austin Public Health, Austin, Texas, 2019. [Online]. Available: https://www.austintexas.gov/sites/default/files/files/Health/Epidemiology/APH_Dockless_Electric_Scooter_Study_5-2-19.pdf

[3] Bird. "Safety." Bird. https://www.bird.co/safety/ (accessed January 3, 2021).

[4] *Code of the Town of Blacksburg*, n.d.

[5] Y. Ranaivo. "Blacksburg Town Council passes regulations for electric scooters." The Roanoke Times. https://roanoke.com/news/local/blacksburg-town-council-passes-regulations-for-electric-scooters/article_e276a26a-8484-5e4b-add1-14efd246603b.html#:~:text=Among%20the%20new%20rules%20passed,such%20as%20the%20Huckleberry%20Trail. (accessed January 3, 2021).

[6] Spin. "Spin Terms of Use." Spin. https://www.spin.app/terms (accessed January 3, 2021).

[7] C. Farrell. "5 Things To Know Before You Ride an Electric Scooter." https://www.santamonica.gov/blog/5-things-to-know-before-you-ride-an-electric-scooter#:~:text=Electric%20scooters%20go%20up%20to,in%20parks%2C%20including%20Palisades%20Park. (accessed January 5, 2021).

[8] Lyft. "Lyft Rideable Rental, Waiver of Liability and Release Addendum." Lyft. https://s3.amazonaws.com/api.lyft.com/static/terms-scooter-bike.html (accessed January 3, 2021).

[9] City of Austin. "Shared Mobility Services." http://austintexas.gov/sharedmobility (accessed January 6, 2021).

[10] City of Charlotte. "E-Scooter Rules & Safety." https://charlottenc.gov/Transportation/Programs/Pages/EScooterSharePilotProgram.aspx#:~:text=NOTE%3A%20All%20e%2Dscooter%20operators,of%20e%2Dscooters%20in%20Charlotte. (accessed January 6, 2021).

[11] T. K. Trivedi *et al.*, "Injuries associated with standing electric scooter use," *JAMA network open*, vol. 2, no. 1, pp. e187381-e187381, 2019.

[12] K. X. Farley *et al.*, "Estimated incidence of electric scooter injuries in the US from 2014 to 2019," *JAMA network open*, vol. 3, no. 8, pp. e2014500-e2014500, 2020.

[13] Skip. "SKIP TERMS OF SERVICE." Skip. https://skipscooters.com/wp-content/uploads/2019/03/SKIP-TERMS-OF-SERVICE_09-07-2018.html (accessed January 3, 2021).

[14] M. Aizpuru, K. X. Farley, J. C. Rojas, R. S. Crawford, T. J. Moore Jr, and E. R. Wagner, "Motorized scooter injuries in the era of scooter-shares: a review of the national electronic surveillance system," *The American Journal of Emergency Medicine*, vol. 37, no. 6, pp. 1133-1138, 2019.

[15] M. Liu, S. Seeder, and H. Li, "Analysis of E-Scooter trips and their temporal usage patterns," *Institute of Transportation Engineers. ITE Journal*, vol. 89, no. 6, pp. 44-49, 2019.
[16] T. J. Puzio *et al.*, "The electric scooter: A surging new mode of transportation that comes with risk to riders," *Traffic Inj Prev*, vol. 21, no. 2, pp. 175-178, 2020, doi: 10.1080/15389588.2019.1709176.
[17] A. Badeau, C. Carman, M. Newman, J. Steenblik, M. Carlson, and T. Madsen, "Emergency department visits for electric scooter-related injuries after introduction of an urban rental program," *The American journal of emergency medicine*, vol. 37, no. 8, pp. 1531-1533, 2019.
[18] I. Shichman, O. Shaked, S. Factor, A. Weiss-Meilik, and A. Khoury, "Emergency department electric scooter injuries after the introduction of shared e-scooter services: A retrospective review of 3,331 cases," *World journal of emergency medicine*, vol. 13, no. 1, p. 5, 2022.
[19] P. S. Fischer, "Understanding and Tackling Micromobility: Transportation's New Disruptor," 2020.
[20] K. C. English *et al.*, "The characteristics of dockless electric rental scooter-related injuries in a large US city," *Traffic injury prevention*, vol. 21, no. 7, pp. 476-481, 2020.
[21] D. Goodman, A. Witte, R.-L. Stark, and A. Frackelton, "E-Scooter management in midsized cities in the United States," 2019.
[22] N. Sikka, C. Vila, M. Stratton, M. Ghassemi, and A. Pourmand, "Sharing the sidewalk: A case of E-scooter related pedestrian injury," *The American journal of emergency medicine*, vol. 37, no. 9, pp. 1807. e5-1807. e7, 2019.
[23] M. B. Bloom *et al.*, "Standing electric scooter injuries: impact on a community," *The American Journal of Surgery*, vol. 221, no. 1, pp. 227-232, 2020.
[24] H. Kleinertz, A. Volk, D. Dalos, R. Rutkowski, K.-H. Frosch, and D. M. Thiesen, "Risk factors and injury patterns of e-scooter associated injuries in Germany," *Scientific reports*, vol. 13, no. 1, p. 706, 2023.
[25] N. R. Shah, S. Aryal, Y. Wen, and C. R. Cherry, "Comparison of motor vehicle-involved e-scooter and bicycle crashes using standardized crash typology," *Journal of safety research*, vol. 77, pp. 217-228, 2021.
[26] A. J. Hawkins. "Bird will give you free scooter rides if you take a selfie while wearing a helmet." The Verge. https://www.theverge.com/2019/11/19/20972447/bird-free-scooter-rides-selfie-wearing-helmet (accessed January 11, 2021).
[27] K. Anderson-Hall, B. Bordenkircher, R. O'Neil, and S. C. Scott, "Governing micro-mobility: A nationwide assessment of electric scooter regulations," 2019.
[28] *Bicycle and Personal Transportation Devices*, V. P. I. a. S. University 5005, 2019.
[29] *Vehicle Code*, 2019.
[30] W. Wei, Y. Petit, P.-J. Arnoux, and N. Bailly, "Head-ground impact conditions and helmet performance in E-scooter falls," *Accident Analysis & Prevention*, vol. 181, p. 106935, 2023.
[31] A. Harbrecht *et al.*, "What to expect? Injury patterns of Electric-Scooter accidents over a period of one year-A prospective monocentric study at a Level 1 Trauma Center," *European Journal of Orthopaedic Surgery & Traumatology*, vol. 32, no. 4, pp. 641-647, 2022.

[32] P. F. Alexandre Coelho, Laura Corominas, Juan Francisco Sanchez-Soler, Daniel Perez-Prieto, Santos Martinex-Diaz, Albert Alier, Jaon Carles Monllau, "Electronic Scooter-Related Injuries: A New Epidemic in Orthopedics," *Journal of Clinical Medicine*, vol. 10(15), 2021, doi: 10.3390/jcm10153283.
[33] H. Stigson, I. Malakuti, and M. Klingegård, "Electric scooters accidents: Analyses of two Swedish accident data sets," *Accident Analysis & Prevention*, vol. 163, p. 106466, 2021.
[34] P. Posirisuk, C. Baker, and M. Ghajari, "Computational prediction of head-ground impact kinematics in e-scooter falls," *Accident Analysis & Prevention*, vol. 167, p. 106567, 2022.
[35] M. Ptak, F. A. O. Fernandes, M. Dymek, C. Welter, K. Brodziński, and L. Chybowski, "Analysis of electric scooter user kinematics after a crash against SUV," *PLOS ONE*, vol. 17, no. 1, p. e0262682, 2022, doi: 10.1371/journal.pone.0262682.
[36] D. Marzougui, R. R. Samaha, C. Cui, C.-D. Kan, and K. S. Opiela, "Extended Validation of the Finite Element Model for the 2010 Toyota Yaris Passenger Sedan," NCAC 2012-W-005, 2012.
[37] P. Ghosh, M. Andersson, M. M. Vazquez, M. Svensson, C. Mayer, and J. Wismans, "A proposal for integrating pre-crash vehicle dynamics into occupant injury protection evaluation of small electric vehicles," presented at the roceedings of IRCOBI Conference, Lyon (France), 2015.
[38] S. Guha, "LSTC_NCAC Hybrid III 50th Dummy," in *Positioning & Post-Processing*, ed. Michigan: LSTC Michigan, 2014.
[39] H. I. Solutions, *Harmonized Hybrid III 50th Male User Manual*, 78051-218-H ed. Humanetics Innovative Solutions, 2017.
[40] P. K. M. S. I. Yi, C.D. Kan, G. J. Park, "Finite element modeling of a Hybrid III dummy and material identification for validation," (in English), *P I Mech Eng D-J Aut*, vol. 225, no. D1, pp. 54-73, 2011, doi: 10.1243/09544070jauto1568.
[41] LSTC, "LS-Dyna Keyword User's Manual," LSTC, 2017, vol. 1.
[42] P. Ghosh, M. Andersson, M. M. Vazquez, M. Svensson, C. Mayer, and J. Wismans, "A proposal for integrating pre-crash vehicle dynamics into occupant injury protection evaluation of small electric vehicles," in *IRCOBI Conference Proceedings*, 2015, no. IRC-15-88.
[43] D. Marzougui, R. R. Samaha, L. Nix, and C.-D. S. Kan, "Extended validation of the finite element model for the 2010 Toyota Yaris passenger sedan (MASH 1100kg vehicle)," 2013.
[44] LSTC, "LS-Dyna Keyword User's Manual, Material Models," LSTC, 2017, vol. 2.
[45] "Oregon Municipal Code." Quality Code Publishing. https://library.qcode.us/lib/port_orford_or/pub/municipal_code/item/title_12-chapter_12_20-12_20_120 (accessed 2022).
[46] K. M. Yates, "Protection of Rear Seat Occupants Using Finite Element Analysis," Virginia Tech, 2020.
[47] N. B. Stander, A.; Roux, W.; Liebold, K.; Eggleston, T.; Goel, T.; Craig, K., "LS-OPT® User's Manual, A Design Optimization and Probabilistic Analysis Tool for The Engineering Analyst," LSTC, Livermore, CA, USA, 2020.
[48] F. R., *Statistical Methods for Research Workers*. Edinburgh: Oliver and Boyd, 1925.
[49] D. Szucs and J. P. Ioannidis, "When null hypothesis significance testing is unsuitable for research: a reassessment," *Frontiers in human neuroscience*, vol. 11, p. 390, 2017.
[50] K. M. Yates, "Protection of Rear Seat Occupants Using Finite Element Analysis," P.h.D., Biomedical Eng. and Mechanics, Virginia Tech, Blacksburg, VA, USA, 2020.

[51] (July 11, 2008). *134, Part II. National Highway Traffic Safety Administration Consumer Information: New Car Assessment Program.*
[52] "MatWeb Material Property of Data." MatWeb. https://www.matweb.com/search/datasheet.aspx?bassnum=MS0001&ckck=1 (accessed 2022).
[53] C. Simms and D. Wood, *Pedestrian and cyclist impact: a biomechanical perspective*. Springer Science & Business Media, 2009.
[54] C. D. Untaroiu, W. Pak, Y. Meng, J. Schap, B. Koya, and S. Gayzik, "A finite element model of a midsize male for simulating pedestrian accidents," *Journal of biomechanical engineering,* vol. 140, no. 1, 2018.
[55] D. Grindle *et al.*, "A detailed finite element model of a mid-sized male for the investigation of traffic pedestrian accidents," *Proc Inst Mech Eng H,* vol. 235, no. 3, pp. 300-313, Mar 2021, doi: 10.1177/0954411920976223.
[56] W. Pak, D. Grindle, and C. Untaroiu, "The influence of gait stance and vehicle type on pedestrian kinematics and injury risk," *Journal of Biomechanical Engineering,* vol. 143, no. 10, 2021.
[57] A. Santacreu, G. Yannis, O. de Saint Leon, and P. Crist, "Safe micromobility," 2020.
[58] T. Bońkowski, J. Špička, and L. Hynčik, "On the simulation of electric scooter crash-test with the hybrid human body model," in *2022 20th International Conference on Emerging eLearning Technologies and Applications (ICETA)*, 2022: IEEE, pp. 59-65.
[59] R. Chontos, D. Grindle, A. Untaroiu, Z. Doerzaph, and C. Untaroiu, "A Finite Element Model of an Electric Scooter for Simulating Traffic Accidents," in *International Design Engineering Technical Conferences and Computers and Information in Engineering Conference*, 2022, vol. 86205: American Society of Mechanical Engineers, p. V001T01A003.
[60] D. Schwartz, B. Guleyupoglu, B. Koya, J. D. Stitzel, and F. S. Gayzik, "Development of a computationally efficient full human body finite element model," *Traffic injury prevention,* vol. 16, no. sup1, pp. S49-S56, 2015.
[61] A. J. Novotny, "Improving E-Scooter Safety: Deployment Policy Recommendations, Design Optimization, and Training Development," Virginia Tech, 2023.
[62] C. Klug *et al.*, "Development of a procedure to compare kinematics of human body models for pedestrian simulations," *IRC-17-64,* 2017.
[63] Y. Peng, J. Yang, C. Deck, and R. Willinger, "Finite element modeling of crash test behavior for windshield laminated glass," *International Journal of Impact Engineering,* vol. 57, pp. 27-35, 2013.
[64] C. Lef and G. Dolange, "Understanding Lower Leg Injury in Offset Frontal Crash: A Multivariate Analysis," ed, 2015.
[65] L. Shi, Y. Han, H. Huang, Q. Li, B. Wang, and K. Mizuno, "Analysis of pedestrian-to-ground impact injury risk in vehicle-to-pedestrian collisions based on rotation angles," *J Safety Res,* vol. 64, pp. 37-47, Feb 2018, doi: 10.1016/j.jsr.2017.12.004.
[66] P. Störmann *et al.*, "Characteristics and injury patterns in electric-scooter related accidents—a prospective two-center report from Germany," *Journal of clinical medicine*, vol. 9, no. 5, p. 1569, 2020. [Online]. Available: https://www.mdpi.com/2077-0383/9/5/1569/htm.

[67] W. Decker, B. Koya, W. Pak, C. D. Untaroiu, and F. S. Gayzik, "Evaluation of finite element human body models for use in a standardized protocol for pedestrian safety assessment," *Traffic injury prevention*, vol. 20, no. sup2, pp. S32-S36, 2019.

[68] E. Song *et al.*, "Reference PMHS Tests to Assess Whole-Body Pedestrian Impact Using a Simplified Generic Vehicle Front-End," in *IRCOBI conference proceedings*, 2017.